Astronomy & Astrophysics manuscript no. T2C_PL_PR
June 19, 2021
©ESO 2021

arXiv:1705.04487v1 [astro-ph.SR] 12 May 2017

The period – luminosity and period – radius relations of Type II and anomalous Cepheids in the Large and Small Magellanic Clouds

M. A. T. Groenewegen[1] and M. I. Jurkovic[2, 3]

[1] Koninklijke Sterrenwacht van België (KSB), Ringlaan 3, B-1180 Brussels, Belgium
e-mail: martin.groenewegen@oma.be
[2] Astronomical Observatory of Belgrade (AOB), Volgina 7, 11 060 Belgrade, Serbia
e-mail: mojur@aob.rs
[3] Konkoly Observatory, Research Centre for Astronomy and Earth Sciences, Hungarian Academy of Sciences, H-1121 Budapest, Konkoly Thege Miklós út 15-17., Hungary

Received ...; accepted ...

ABSTRACT

Context. Type II Cepheids (T2Cs) and anomalous Cepheids (ACs) are pulsating stars that follow separate period-luminosity relations.
Aims. We study the period-luminosity (*PL*) and period-radius (*PR*) relations for T2Cs and ACs in the Magellanic Clouds.
Methods. In an accompanying paper we determined luminosity and effective temperature for the 335 T2Cs and ACs in the LMC and SMC discovered in the OGLE-III survey, by constructing the spectral energy distribution (SED) and fitting this with model atmospheres and a dust radiative transfer model (in the case of dust excess). Building on these results we study the *PL*- and *PR* relations. Using existing pulsation models for RR Lyrae and classical Cepheids we derive the period-luminosity-mass-temperature-metallicity relations, and then estimate the pulsation mass.
Results. The *PL* relation for the T2Cs does not appear to depend on metallicity, and, excluding the dusty RV Tau stars, is $M_{\rm bol} = +0.12 - 1.78 \log P$ (for $P < 50$ days). Relations for fundamental and first overtone LMC ACs are also presented. The *PR* relation for T2C also shows little or no dependence on metallicity or period. Our preferred relation combines SMC and LMC stars and all T2C subclasses, and is $\log R = 0.846 + 0.521 \log P$. Relations for fundamental and first overtone LMC ACs are also presented. The pulsation masses from the RR Lyrae and classical Cepheid pulsation models agree well for the short period T2Cs, the BL Her subtype, and ACs, and are consistent with estimates in the literature, i.e. $M_{\rm BLH} \sim 0.49\ M_{\odot}$ and $M_{\rm AC} \sim 1.3\ M_{\odot}$, respectively. The masses of the W Vir appear similar to the BL Her. The situation for the pWVir and RV Tau stars is less clear. For many RV Tau the masses are in conflict with the standard picture of (single-star) post-AGB evolution, the masses being either too large ($\gtrsim 1\ M_{\odot}$) or too small ($\lesssim 0.4\ M_{\odot}$).

Key words. stars: variables: Cepheids: Type II Cepheids — stars: variables: Cepheids: Anomalous Cepheids — stars: fundamental parameters — Magellanic Clouds — stars: distances

1. Introduction

Type II Cepheids (T2Cs) and anomalous Cepheids (ACs) are pulsating stars located in the instability strip (IS) of the Hertzsprung-Russell diagram (HRD) also occupied by the classical Cepheids (CCs) and RR Lyrae (RRL) variables. T2C are classically divided into subgroups based on their period, and, following Soszyński et al. (2008b) and Soszyński et al. (2010b), they are the BL Herculis (BLH) (1−4 days), the (peculiar) W Virginis ((p)WVir) (4 – 20 days), and the RV Tauris (RVT) (20 – 70 days). The pulsation period of the ACs (from ∼ 0.9 to ∼ 2 days) overlaps with the short period T2Cs. T2Cs are known to pulsate in fundamental mode (FU) only, while the ACs pulsate in the first overtone (FO) and fundamental mode (FU).

An important characteristic of T2Cs and ACs is that they follow a period-luminosity (*PL*) relation, and that these objects can be found in globular clusters, and galaxies (Catelan & Smith 2015). They can therefore be used in the calibration of the distance scale. T2Cs in particular are useful where CCs are too few and RRL too faint (see for example the review by Sandage & Tammann (2006) and Wallerstein (2002)). ACs fill a space on the *PL*-diagram above the RRL and T2Cs by ∼0.5 to ∼2 magnitudes (as the period increases), but do not reach into the CC region. Caputo et al. (2004) investigated the possibility that they do continue to the *PL* relation of CCs, but Fiorentino & Monelli (2012) concluded that they are metal-poor stars that would not evolve into the CC IS region.

Period - luminosity relations have been discussed in several papers over the past decades. Nemec et al. (1994) is a rare example were $P - L$−[Fe/H] relations are derived for T2Cs and ACs (as well as RRL and SX Phe stars) in (B, V, K) colours based on objects in globular clusters. Recently, Clementini et al. (2016) presented *PL* relations for T2Cs and FU and FO ACs in the *Gaia G*-band. Marconi et al. (2004) provided a theoretical mass-dependent Period-Magnitude-Colour (PMC), Period-Wesenheit (PW) and Period-Magnitude-Amplitude relations for ACs in the metallicity range $Z = 0.0001 - 0.0004$. They also give the empirical $PW(VI)$ relation based on ACs observed in 7 dwarf spheroidal galaxies. Ripepi et al. (2014), as a part of the VISTA Magellanic Cloud (VMC) Survey (Cioni et al. 2011), provided the *PL* relation in the $K_{\rm s}$ band, and the $PW(V, K)$ relation for FU and FO ACs in the LMC, as well as the *PL* relation in the *V* and *I* band, a *PMC* and the $PW(V, I)$ relation based on the original OGLE-data.

Di Criscienzo et al. (2007) derived theoretical period-magnitude (*PM*) in the NIR and period-Wesenheit (*PW*) for various optical and NIR colour combinations relations combining pulsation models and evolutionary tracks for stars with periods up to 8 days, i.e. BLHs. Matsunaga et al. (2011) present NIR *PL* relations and Wesenheit relations for T2C in the SMC, and compare the results to their earlier work on the LMC (Matsunaga et al. 2009) and Galactic Centre (GC) (Matsunaga et al. 2006). The *K*-band *PL* relation for T2C in the GC was also presented by Groenewegen et al. (2008), and the absolute calibration was considered by Feast et al. (2008). More recently, Manick et al. (2017) used the OGLE-III LMC T2Cs to derive the Wesenheit *PW* relation.

Recent survey work in the NIR allowed a reappraisal of the *PL* relations, notably, Ripepi et al. (2015) considered VMC data (Cioni et al. 2011) to present several *PL*, *PLC* and *PW* relations, while Bhardwaj et al. (2017) did a similar study using NIR data from the LMC Synoptic Survey (Macri et al. 2015).

Apparently, there has been little recent work done on the radii of T2Cs. Burki & Meylan (1986) give a period-radius (*PR*) relation based on older data, and Balog et al. (1997) derived the radii for 17 Galactic T2Cs using the Baade-Wesselink method. Figure 5 in their article displays a *PR* relation, but they did not give an equation for their fit.

Masses for the T2Cs were estimated by Bono et al. (1997a) to be in a range between 0.52 and 0.59 $M_{\odot}$ (for $Z < 0.001$) for stars with periods below 15 days. Quoting the results of Vassiliadis & Wood (1993), Wallerstein (2002) gives the initial mass of the brighter T2Cs (the RVT) to be around 1 $M_{\odot}$. In the case of ACs pulsation models have been considered by various authors to find masses in the range 1.3-2.2 $M_{\odot}$ (for $Z = 0.0001$ and 0.0004, Bono et al. (1997b), Marconi et al. (2004)), or, specifically 1.2 ± 0.2 $M_{\odot}$ for the ACs in the LMC (Fiorentino & Monelli 2012). Recently, Martínez-Vázquez et al. (2016) find ~ 1.5 $M_{\odot}$ for four ACs in the Sculptor dSph galaxy.

In the accompanying paper, (Groenewegen & Jurkovic (2017), hereafter GJ17) studied all 335 T2C and AC in the Small and Large Magellanic Clouds (MCs) detected in the OGLE-III data (Soszyński et al. (2008b), Soszyński et al. (2010b), Soszyński et al. (2010a)[1]). The spectral energy distributions (SEDs) were constructed using photometry from the literature and fitted with the dust radiative transfer code "More of DUSTY" (MoD, Groenewegen (2012)), an extension of the DUSTY radiative transfer code DUSTY (Ivezić et al. 1999). Luminosities and effective temperatures were derived and are given in the Appendix in GJ17. The resulting Hertzsprung-Russell diagram was compared in a qualitative way to modern evolutionary tracks. In agreement with the findings cited above the BL Her can be explained by stars in the mass range $\sim 0.5 - 0.6$ $M_{\odot}$ and the ACs by stars in the mass range $\sim 1.1 - 2.3$ $M_{\odot}$. The origin of the (p)WVir is unclear however: tracks of $\sim 2.5 - 4$ $M_{\odot}$ cross the IS at the correct luminosity, as well as (some) lower mass stars on the AGB that undergo a thermal pulse when the envelope mass is small, but the timescales make these unlikely scenarios.

For $\sim$ 60% of the RVT and $\sim$ 10% of the W Vir (including the pWVir) objects an infrared excess was detected from the SED fitting. The results of Kamath et al. (2016) were confirmed that there exist stars with luminosities below that predicted from single-star evolution that show a clear infrared excess. The light curves of more than 130 systems were investigated to look for the light-travel time (LTT) effect or light-time effect (LITE) (Irwin 1952) in so-called *observed minus calculated*, (O-C)-diagrams. Twenty possible new binaries were identified, and about 40 stars that show a significant period change.

Previous work concentrated almost exclusively on deriving the *PL* relation in the NIR bands or using the Wesenheit index, the main aim of this paper is to use the stellar luminosity as parameter and in that way study the properties of these stars in a more fundamental way. We used the results published in GJ17 to derive the period-luminosity and *PR* relations of T2Cs and ACs. In addition, we derive estimates of the masses of these stars, based on theoretical pulsation models of RRL and CCs.

In Section 2 we discuss the derived *PL* relations for T2Cs and ACs. In Section 3 the period-radius relation is presented, and in Section 4 we estimate the masses. In the Section 5 we discuss and summarise our findings.

2. Period – Luminosity relation

Figure 1 first shows the classical *PL* relation using the Wesenheit magnitude, $W = I - 1.55 \cdot (V - I)$, combining Fig. 1 in Soszyński et al. (2008b) and Fig. 1 in Soszyński et al. (2010b). In GJ17 we used distances to the LMC and SMC of 50 and 61 kpc in the SED modelling, and therefore we shifted the magnitudes of the SMC objects by 0.432 mag (distance moduli, DM, 18.927-18.495) to put them on the magnitude scale of the LMC. The most prominent outliers are marked with their identifier.

Wesenheit *PL* relations have been derived for various combinations of subclasses of T2Cs and ACs for both the LMC and SMC, and combined ("@LMC", meaning the SMC objects have been placed at the distance of the LMC) and the results are listed in Table 1. Stars showing eclipsing or ellipsoidal variation (as identified by OGLE; the blue crosses in Figure 1) have been excluded in the fitting and iterative 3σ clipping has been applied to remove outliers.

Table 1, in addition, includes other determinations of the Wesenheit *PL* relation from the literature, both observational as theoretical. The Wesenheit *PL* relation does not not seem to depend on metallicity. At characteristic periods of $\log P = 0.5$ (BLH), 1.5 (RVT) and 1.0 (WVir, and the solutions that include BLH and/or RVT) the magnitude difference between the solutions for the SMC and LMC are within the errors consistent with the expected difference of 0.43 mag.

The derived relations are also in agreement with those listed in the literature although this is not so surprising as there are all based on the same OGLE-III data and only differ in details. The RVT stars that show IR excess are brighter in W than those without (also remarked by Manick et al. (2017)), but excluding those there is well defined $W(VI)$ relation for BLH, WVIR and non-dusty RVT, as illustrated in Figure 1.

The agreement with theoretical models is good for the BLH. The comparison with observations requires an adopted distance to the LMC, and an assumed metallicity for the models. For [Fe/H]= -1 and DM= 18.50 theory and observations agree within the error. The agreement is less good for the ACs, in particular the theoretical slope differs by almost 3σ from the empirically derived one.

Figure 2 shows the bolometric version of the *PL* relation, using the luminosities derived in GJ17. The bottom part of Table 1 gives the corresponding fits to the *PL* relation. What is immediately noticeable is that the scatter in the bolometric *PL*

[1] Soszyński et al. (2010a) originally listed the 6 SMC ACs with a classical Cepheid identification number. In the OGLE-III Variable Stars Database (http://ogledb.astrouw.edu.pl/~ogle/CVS/ they were subsequently listed under the names that we use in GJ17 and the present paper, OGLE-SMC-ACEP 01...06.

Table 1. Wesenheit and bolometric period-luminosity relations.

Sample	Galaxy[a]	Mag	Mag=	a	$+b \log P$	dispersion (mag)	χ^{2b}_r	N	N outliers	Ref.
BL Her	LMC	W	17.359 ± 0.022	-2.576 ± 0.080		0.089	9.18	55	6	
BL Her	SMC	W	17.558 ± 0.134	-2.429 ± 0.480		0.241	76.0	17	0	
BL Her	@LMC	W	17.347 ± 0.038	-2.669 ± 0.137		0.170	32.8	74	4	
W Vir	LMC	W	17.402 ± 0.064	-2.558 ± 0.063		0.093	9.91	76	2	
W Vir	SMC	W	18.329 ± 0.168	-3.009 ± 0.158		0.091	11.5	10	0	
W Vir	@LMC	W	17.471 ± 0.061	-2.624 ± 0.060		0.098	10.8	86	2	
RV Tau	LMC	W	18.101 ± 0.557	-3.142 ± 0.352		0.249	72.6	41	1	
RV Tau	SMC	W	17.707 ± 1.049	-2.585 ± 0.674		0.164	42.1	7	0	
RV Tau	@LMC	W	18.004 ± 0.494	-3.077 ± 0.313		0.240	66.9	48	1	
BL Her + W Vir	LMC	W	17.363 ± 0.017	-2.522 ± 0.021		0.102	11.6	133	6	
BL Her + W Vir	SMC	W	17.597 ± 0.072	-2.356 ± 0.103		0.209	53.0	26	1	
BL Her + W Vir	@LMC	W	17.335 ± 0.017	-2.496 ± 0.021		0.108	13.2	153	13	
BL Her + W Vir + RV Tau[c]	LMC	W	17.358 ± 0.014	-2.530 ± 0.017		0.089	9.00	136	10	
BL Her + W Vir + RV Tau[c]	SMC	W	17.577 ± 0.073	-2.388 ± 0.097		0.232	64.9	28	0	
BL Her + W Vir + RV Tau[c]	@LMC	W	17.355 ± 0.017	-2.526 ± 0.020		0.118	15.8	162	12	
AC FU	LMC	W	16.612 ± 0.020	-3.158 ± 0.141		0.150	25.7	62	0	
AC FO	LMC	W	16.029 ± 0.058	-3.373 ± 0.247		0.140	24.2	19	0	
BL Her + W Vir	LMC	W	17.364 ± 0.015	-2.521 ± 0.022		0.105		131		1
BL Her + W Vir	SMC	W	17.554 ± 0.083	-2.304 ± 0.107		0.230		27		2
BL Her + W Vir + RV Tau[d]	LMC	W	17.33 ± 0.03	-2.53 ± 0.03						3
BL Her	Theory	W	17.30 ± 0.07	-2.43 ± 0.02						4
AC FU	LMC	W	16.59 ± 0.02	-3.41 ± 0.16		0.15				5
AC FO	LMC	W	16.05 ± 0.05	-3.44 ± 0.22		0.13				5
AC FU	Theory	W	16.55	-2.94						6
BL Her	LMC	$M_{\rm bol}$	$+0.141 \pm 0.051$	-1.749 ± 0.200		0.274	33.0	57	4	
BL Her	SMC	$M_{\rm bol}$	-0.250 ± 0.176	-0.691 ± 0.717		0.302	64.9	15	2	
BL Her	MCs	$M_{\rm bol}$	-0.027 ± 0.065	-1.326 ± 0.257		0.282	89.5	72	6	
W Vir	LMC	$M_{\rm bol}$	0.723 ± 0.115	-2.358 ± 0.119		0.186	36.8	74	5	
W Vir	SMC	$M_{\rm bol}$	0.965 ± 0.318	-2.589 ± 0.319		0.210	33.2	10	0	
W Vir	MCs	$M_{\rm bol}$	0.743 ± 0.109	-2.379 ± 0.112		0.201	37.1	85	4	
RV Tau[d]	LMC	$M_{\rm bol}$	$+1.442 \pm 1.146$	-2.919 ± 0.750		0.301	91.1	15	0	
RV Tau[d]	SMC	$M_{\rm bol}$	-1.088 ± 0.433	-1.367 ± 0.290		0.041	4.6	4	0	
RV Tau[d]	MCs	$M_{\rm bol}$	$+0.951 \pm 0.974$	-2.620 ± 0.639		0.298	78.4	19	0	
BL Her + W Vir	LMC	$M_{\rm bol}$	$+0.199 \pm 0.035$	-1.827 ± 0.042		0.230	40.6	130	10	
BL Her + W Vir	SMC	$M_{\rm bol}$	-0.087 ± 0.100	-1.561 ± 0.182		0.349	256.	26	1	
BL Her + W Vir	MCs	$M_{\rm bol}$	$+0.068 \pm 0.037$	-1.704 ± 0.049		0.267	83.1	159	8	
BL Her + W Vir + RV Tau[c]	LMC	$M_{\rm bol}$	$+0.226 \pm 0.033$	-1.870 ± 0.039		0.233	40.5	136	11	
BL Her + W Vir + RV Tau[c]	SMC	$M_{\rm bol}$	-0.048 ± 0.101	-1.686 ± 0.172		0.370	275.	27	1	
BL Her + W Vir + RV Tau[c, e]	MCs	$M_{\rm bol}$	$+0.119 \pm 0.036$	-1.787 ± 0.044		0.276	81.8	166	9	
AC FU	LMC	$M_{\rm bol}$	-0.436 ± 0.033	-3.122 ± 0.213		0.255	71.3	61	1	
AC FO	LMC	$M_{\rm bol}$	-1.126 ± 0.074	-3.248 ± 0.305		0.244	53.2	20	0	

References. (1) Matsunaga et al. (2009); (2) Matsunaga et al. (2011); (3) Manick et al. (2017); (4) Di Criscienzo et al. (2007) for [Fe/H] = −1, $l/H_{\rm p}$ = 1.5, and LMC distance modulus 18.50; (5) Ripepi et al. (2014) ; (6) Marconi et al. (2004) for M = 1.3 $M_{\odot}$and LMC distance modulus 18.50.

Notes. [(a)] For the *PL* relations in the Wesenheit index "@LMC" means the stars in the LMC plus the stars in the SMC placed at the distance of the LMC by a shift of 0.432 magnitude. [(b)] The reduced χ^2 is based on an assumed "error" in the Wesenheit index and bolometric magnitude of 0.03 mag. [(c)] Excluding RVTs with dust excess and for $P < 50$ days. [(d)] Excluding RVTs with dust excess. [(e)] The preferred solution.

relations is significantly larger than in the corresponding Wesenheit relations. There could be several reasons for this. First, the Wesenheit relations are based on two intensity-mean magnitudes, while the luminosities are derived based on a fit to the entire SED, that is based on non-contemporaneous photometry. Second, if there are issues related to blending or binarity then certain combinations of the parameters involved may still yield a Wesenheit index close to the mean relation, but the fitting of the entire SED will more likely yield deviant results.

For comparison we will refer to two other systems throughout the discussion, namely the best studied of the known CCs in an eclipsing binary in the LMC (OGLE-LMC-CEP-0227), and one of the best studied T2C in our Galaxy, κ Pav (WVir type, P = 9.09 days). The latter has a HST-based distance of 180 ± 9 pc (Benedict et al. 2011) and a metallicity of [Fe/H]=

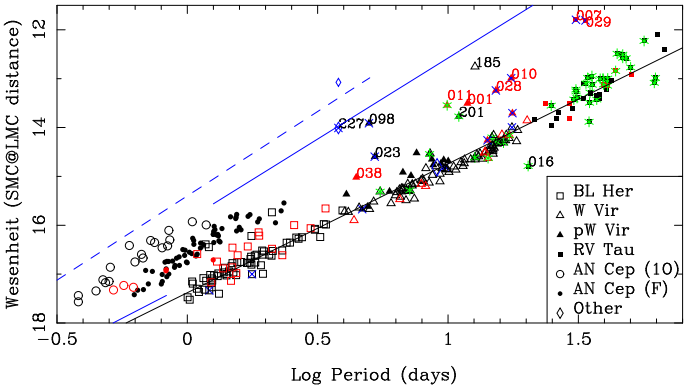

Fig. 1. The Wesenheit *PL* relation. Stars in the SMC are plotted in red, and shifted to the distance of the LMC. Some outliers are marked with their identifier. Stars with an IR excess according to GJ17 are marked by a green plus sign. Stars that show eclipsing or ellipsoidal variations according to OGLE are marked by a blue cross. Stars plotted as a blue diamond are OGLE-LMC-CEP-0227 (the classical Cepheid in an eclipsing binary system, at $P = 3.79$ days), and the Galactic T2C κ Pav (at $P = 9.08$ days), scaled to the distance of the LMC, see text. For -0227 both the system value is plotted (the smaller, brighter point), and the Wesenheit magnitude of the Cepheid in the system (from Pilecki et al. (2013)). The black solid line is the relation derived from the BLH + WVIR + non-dusty RVTs with periods below 50 days in the LMC (see Table 1), plotted over the entire period range. The blue lines indicate the Wesenheit relation for CC in the LMC from Soszyński et al. (2008a) for FU (solid line) and FU (dashed line) pulsators, and the relation for RRab stars (at $\log P < -0.08$) from Soszynski et al. (2003).

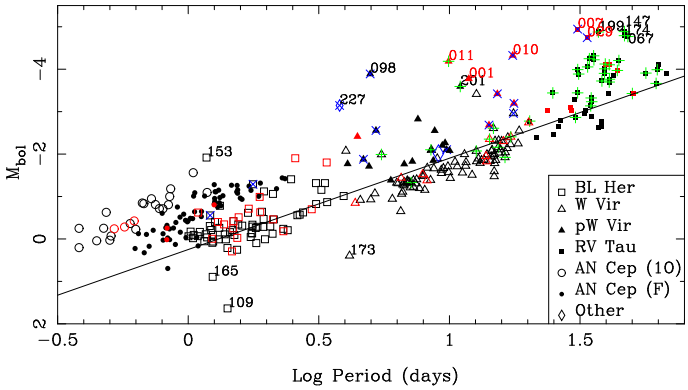

Fig. 2. Bolometric *PL*−relation. Stars in the SMC are plotted in red. The error in $M_{\rm bol}$ is smaller than the plot symbol. Some outliers are plotted with their identifier. Stars with an IR excess according to GJ17 are marked by a green plus sign. Stars that show eclipsing or ellipsoidal variations according to OGLE are marked by a blue cross. The classical Cepheid in the eclipsing binary OGLE-LMC-CEP-0227 (at $P = 3.79$ days) and the Galactic T2C κ Pav (at $P = 9.08$ days) are plotted as blue diamonds. The black solid line is the relation derived from the BLH + WVIR + non-dusty RVTs with periods below 50 days in the LMC (see Table 1), plotted over the entire period range.

0.0 (Luck & Bond 1989). It is not listed in the 1st *Gaia* data release (Gaia Collaboration et al. 2016). Time-series photometry in V, I is available from Berdnikov (2008), from which we derived the mean magnitudes. In Figure 1 it is plotted as if it were located at the adopted distance to the LMC. Breitfelder et al. (2015) quote an effective temperature of $T_{\rm eff} = 5739 \pm 107$ K, implying $L = 508 \pm 65\ L_{\odot}$. Pilecki et al. (2013) have derived the V, I magnitudes of the two components in OGLE-LMC-CEP-0227, and the Wesenheit magnitude of the Cepheid in the system and of the total binary system are plotted in Figure 1 (at $P = 3.79$d), together with the Wesenheit relation for FU and FO CCs in the LMC from Soszyński et al. (2008a). Pilecki et al. (2013) also derived $\log L = 3.158 \pm 0.049\ L_{\odot}$and $T_{\rm eff} = 6050 \pm 160$ K, in agreement with Marconi et al. (2013) ($\log L = 3.16 \pm 0.02\ L_{\odot}$, $T_{\rm eff} = 6100 \pm 50$ K).

κ Pav, that is close to the estimated *PL* relation in the Wesenheit index, is brighter than the relation in bolometric magnitude. The derived radius and effective temperature (Breitfelder et al. 2015) imply $M_{\rm bol} = -2.01 \pm 0.13$ while the various *PL* relations gives values in the range −1.53 to −1.59. This could be due to the intrinsic width of the IS, the assumed distance (although the HST-based distance is accurate to 5%), a metallicity dependence of the *PL* relation (this is not obvious from a comparison of LMC and SMC objects), or the fact that it has a binary companion. In fact, Matsunaga et al. (2009) discusses κ Pav in detail, and suggests that it should be classified as a pWVir object.

The outliers that are marked in both figures are mostly pWVir type stars, some of which have been classified as binaries by the OGLE team: OGLE-LMC-T2CEP-098, and -023, OGLE-SMC-T2CEP-007, -010, -028, or where the LITE was tentatively detected in GJ17, OGLE-SMC-T2CEP-001, and -029. The other outliers are mostly dusty objects with infrared excess detected in GJ17 namely some pWVir objects (OGLE-LMC-T2CEP-201 and OGLE-SMC-T2CEP-011) and mostly RVT (OGLE-LMC-T2CEP-016, -067, -147, -174, -199).

3. Period – Radius relation

Figure 3 shows the *PR* relation based on the derived effective temperatures and luminosities in GJ17. The resulting radii with error bars are given in Table A.

PR relations have been derived for various combinations of the T2C subclasses in the SMC, LMC, and both, and for the FU and FO ACs in the LMC and the results are listed in Tab. 2. Stars showing eclipsing or ellipsoidal variation have been excluded in the fitting and iterative 3σ clipping has been applied to remove outliers. Contrary to the *PL* relations where the dusty RVT stars deviated significantly and where excluded this is not the case here.

Marconi et al. (2015) present the latest nonlinear, time-dependent convective hydrodynamical models of RRL stars for different metallicites and masses. Specifically they present Period-Mass-Radius-Metallicity (PMRZ) relations for fundamental and first-overtone pulsators (Their Eqs. 7 and 8). As they were concerned with RRL they excluded "the sequence D models" (see Marconi et al. (2015) for details) in their fitting procedure, since these luminosity levels were considered too bright for typical RRLs. However, these luminosities are typical for T2C, and therefore we re-derived the PMRZ relation for all models with $\log L > 1.65\ L_{\odot}$ (and that reach up to $\log L \sim 2.0$, and periods up to ~ 2.4 days) using their dataset. We find:

$$\log R = (0.763 \pm 0.003) - (0.037 \pm 0.001) \log Z + (0.560 \pm 0.004) \log P \quad (\mathrm{N} = 195) \quad (1)$$

for FU pulsators, and

$$\log R = (0.855 \pm 0.005) - (0.034 \pm 0.001) \log Z + (0.585 \pm 0.007) \log P \quad (\mathrm{N} = 63) \quad (2)$$

for FO pulsators. These relations are plotted in Fig. 3 at the average metallicity of RRL in the LMC (Gratton et al. 2004) of [Fe/H] = −1.5 (or $\log Z = -3.23$). The theoretical relation lies

above the observed one. The slope agrees within the error bar with the observed relation for BLH (see Table. 2), but the zero point is slightly larger.

In a similar way, Bono et al. (2000) present non-linear pulsation models for CCs for various masses and metallicities. Period-Radius relations for FU pulsators at three different metallicities were already presented in Bono et al. (1998). Here we have re-derived the PMRZ relations for FU and FO pulsators from the Bono et al. (2000) dataset, combining the "canonical" and "non-canonical" models (like they did), and find

$$\log R = (1.115 \pm 0.012) - (0.039 \pm 0.005) \log Z + (0.653 \pm 0.003) \log P \quad (\mathrm{N} = 202) \quad (3)$$

for FU pulsators, and

$$\log R = (1.257 \pm 0.028) - (0.003 \pm 0.014) \log Z + (0.706 \pm 0.016) \log P \quad (\mathrm{N} = 27) \quad (4)$$

for FO pulsators. These relations are plotted in Fig. 3 at the average metallicity of Cepheids in the LMC (Romaniello et al. 2008) of [Fe/H] = −0.33 (or $\log Z = -2.06$).

For comparison we have plotted objects with known radii. The values for the Cepheid in OGLE-LMC-CEP-0227 and Galactic T2C κ Pav are plotted as blue diamonds. Based on a Baade-Wesselink type analysis. Breitfelder et al. (2015) derived a projection factor of $p = 1.26 \pm 0.04 \pm 0.06$, and a radius of $R = 22.83 \pm 1.14\,R_{\odot}$. Big light-blue stars represent Galactic Type II Cepheids that had their radii derived by Balog et al. (1997) using the Baade-Wesselink method. In case of κ Pav ($R = 19 \pm 5\,R_{\odot}$) their result is in good agreement with Breitfelder et al. (2015). It must be noted that since the article was published in 1997, some of the objects have been reclassified. That explains why they scatter so much. Looking at the classification by the General Catalog of Variable Stars (GCVS)[2] and the International Variable Star Index (VSX)[3] it appears that KL Aql (P= 6.1 day), V733 Aql (P= 6.2), BB Her (P= 7.5) and DR Cep (P= 19.1) are CCs. DQ And (P= 3.2) has a questionable classification, but it is more likely than not that is a CCs, too. The cases of TX Del (P= 6.2) and IX Cas (P= 9.1) are different, because their radius from the Baade-Wesselink analysis might have been influenced with the fact that they are in binary systems. AU Peg (P= 2.4) is hard to interpret, because it was suggested that it might not be a T2C, and the radius of $19 \pm 4\ R_{\odot}$ puts it above the *PR* relation for T2Cs. It is also a binary, so, again, that could have had an influence on the determined radius. BL Her (P= 7.5), XX Vir (P= 1.3), SW Tau (P=1.6), NW Lyr (P=1.6), V553 Cen (P= 2.1, a C-rich object), κ Pav, AL Vir (P= 10.3), W Vir (P= 17.3) and V1181 Sgr (P= 21.3) are T2Cs, and they follow our *PR* relation.

There is no obvious dependence of the *PR* relation on metallicity, or on subclass. Within the error bars, all T2C can be represented by a single *PR* relation (solutions 13-15). For this type of relation the slope between the solution for SMC and LMC stars differ by 2σ, but slope and zero point are not independent. At the characteristic period of 10 days the predicted radii for an SMC and LMC T2C are identical. Combining both galaxies and all periods, solution (15) becomes our preferred *PR* relation for T2Cs.

Table 2 also includes the old relation presented in Burki & Meylan (1986). They did not give error bars, but at face value the relation is similar to the preferred relation we derive for the MC T2Cs. Together with the T2C from Balog et al. (1997) this supports the suggestion that there is no strong dependence of the *PR* relation on metallicity.

[2] http://www.sai.msu.su/gcvs/gcvs/
[3] https://www.aavso.org/vsx/

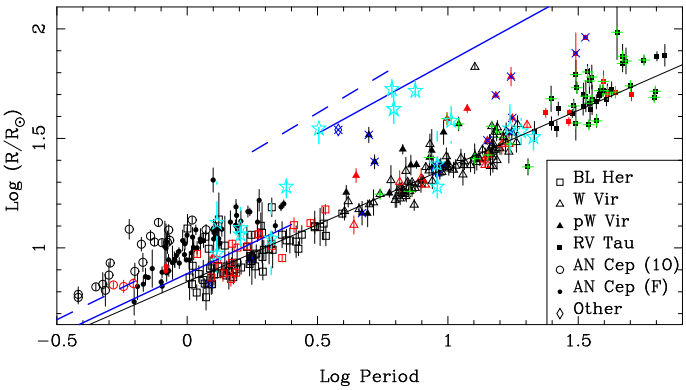

Fig. 3. The Period-radius relation. Stars in the SMC are plotted in red. The black solid line is a fit to the BL Her, W Vir and RV Tau stars in the LMC (excluding 3σ outliers). The blue solid and dashed lines are the theoretical *PR* relations for FU and FO RRL (shorter periods) and CC in the LMC, respectively (see text). The values for the Cepheid in the eclipsing binary system OGLE-LMC-CEP-0227 (at $P = 3.79$ days) and the Galactic T2C κ Pav (at $P = 9.08$ days) are plotted as blue diamonds. Light blue stars are represent the stars from Balog et al. (1997). Details about these stars are given in the text.

4. Masses from evolutionary models

Following Section 3 we derived the following equation for FU pulsators from the models in Marconi et al. (2015) with $\log L > 1.65$,

$$\log P = (11.468 \pm 0.049) + (0.8627 \pm 0.0028) \log L - (0.617 \pm 0.015) \log M - (3.463 \pm 0.012) \log T_{\rm eff} + (0.0207 \pm 0.0013) \log Z \quad (\mathrm{N} = 195, \sigma = 0.0044). \quad (5)$$

Similarly, we used the models in Bono et al. (2000) to find for FU pulsators (cf. their Table 6),

$$\log P = (10.649 \pm 0.085) + (0.9325 \pm 0.0053) \log L - (0.799 \pm 0.020) \log M - (3.282 \pm 0.022) \log T_{\rm eff} + (0.0393 \pm 0.0026) \log Z \quad (\mathrm{N} = 202, \sigma = 0.0085) \quad (6)$$

Equations 5 and 6 allow us to derive the current mass if we know period, luminosity, effective temperature and metallicity. The procedure seems to give sensible results. For the stellar parameters derived for the CC -0227 (Pilecki et al. 2013), and its metallicity of $Z = 0.004$ (Marconi et al. 2013), the equation based on the Cepheid models gives a mass of $4.41 \pm 0.44\,M_{\odot}$, in agreement with the masses found by Pilecki et al. (2013) ($4.165 \pm 0.032\,M_{\odot}$) and Marconi et al. (2013) ($4.14 \pm 0.06\,M_{\odot}$). However, the equation from the RRL pulsation modes also gives an estimate that is correct within the error bar, namely $5.86 \pm 1.18\,M_{\odot}$.

We used Equations 5 and 6 with $Z = 0.004$ (for both LMC and SMC) to estimate the masses. For the overtone AC the equations were evaluated at their fundamental period $\log P_{\rm FU} = \log P_{\rm FO} + 0.127$. Errors were estimated from the error in $T_{\rm eff}$ and L, and the intrinsic scatter in the relation. The results are given in Table A.1. The Cepheid and RRL-based masses agree within 3× the combined error bars (marked as "OK" in Table A.1) or within 15% irrespective of the error bars (marked as "ok" in Table A.1) in 90% for the BLH (72/80), 82% for the FU ACs (53/65), 74% for the FO ACs (17/23), 58% for the pWVir (17/24), but only 22% for the WVir (20/90) and 18% (9/51) for the RVT.

Table 2. Period-Radius relations.

Sample	Galaxy	$\log R = a$ ($R_\odot$)	$+b \log P$	dispersion	χ^2_r	N	N outliers	Solution	Ref.
BL Her	LMC	0.830 ± 0.013	0.564 ± 0.049	0.047	2.60	57	4	(1)	
BL Her	SMC	0.852 ± 0.028	0.574 ± 0.117	0.056	12.4	17	0	(2)	
BL Her	MCs	0.847 ± 0.013	0.551 ± 0.052	0.058	5.43	76	2	(3)	
W Vir	LMC	0.823 ± 0.020	0.541 ± 0.021	0.037	1.74	77	2	(4)	
W Vir	SMC	0.709 ± 0.079	0.620 ± 0.071	0.038	4.11	10	0	(5)	
W Vir	MCs	0.828 ± 0.020	0.531 ± 0.020	0.037	2.25	87	2	(6)	
RV Tau	LMC	0.848 ± 0.141	0.528 ± 0.088	0.076	5.72	41	1	(7)	
RV Tau	SMC	0.977 ± 0.188	0.440 ± 0.124	0.039	2.54	7	0	(8)	
RV Tau	MCs	0.864 ± 0.112	0.517 ± 0.071	0.072	5.16	48	1	(9)	
BL Her + W Vir	LMC	0.837 ± 0.007	0.528 ± 0.008	0.041	2.09	134	6	(10)	
BL Her + W Vir	SMC	0.869 ± 0.015	0.480 ± 0.022	0.050	9.81	27	0	(11)	
BL Her + W Vir	MCs	0.852 ± 0.006	0.508 ± 0.008	0.044	3.46	161	6	(12)	
BL Her + W Vir + RV Tau	LMC	0.833 ± 0.007	0.535 ± 0.007	0.050	2.82	174	8	(13)	
BL Her + W Vir + RV Tau	SMC	0.861 ± 0.013	0.501 ± 0.016	0.050	8.75	34	0	(14)	
BL Her + W Vir + RV Tau[a]	MCs	0.846 ± 0.006	0.521 ± 0.006	0.053	3.91	209	7	(15)	
AC FU	LMC	0.972 ± 0.005	0.692 ± 0.034	0.045	2.39	61	1	(16)	
AC FO	LMC	1.113 ± 0.016	0.733 ± 0.073	0.054	3.65	20	0	(17)	
T2C	Galactic	0.87	0.54						(1)

References. (1) Burki & Meylan (1986).

Notes. [(a)] The preferred solution.

The effect of changing the metallicity was investigated. As a test it was lowered to $Z = 0.0012$ that would give a mass for the Cepheid -0227 from the Cepheid models in agreement with the observations (see above). This improved the agreement between the two mass estimates for the BLH and WVir, slightly reduced the agreement for the FU ACs and left the other percentages unchanged.

For the estimates based on $Z = 0.004$ the geometric mean of the two estimates was taken. For the various pulsation classes we find the following range in masses (listed are the 10,50,90% percentiles), where known eclipsing and ellipsoidal variables were excluded: BL Her (0.36, 0.49, 0.87 $M_\odot$), W Vir (0.31, 0.41, 0.57 $M_\odot$), pW Vir (0.37, 0.74, 1.29 $M_\odot$), RV Tau (0.25, 0.43, 0.82 $M_\odot$), and ACs (0.89, 1.29, 1.90 $M_\odot$), with the same range for FU and FO pulsators. Assuming $Z = 0.0012$ would lower these mass estimates by about 5%. For the RVT it does not matter significantly whether one separates them into the dusty or non-dusty ones.

Taking only the stars where the two mass estimates agree (the "OK" and "ok" from Table A.1) leaves these ranges essentially unchanged for the BLH and the ACs. For the WVir the range becomes (0.43, 0.50, 0.66 $M_\odot$ based on 20 stars). The pWVir have been suggested to be in binary systems. Including eclipsing/ellipsoidal stars, and taking the stars where the two mass estimates agree the mass range is increased significantly to (0.72, 1.22, 1.77 $M_\odot$, for 14 stars). The number of RVT where the two mass estimates agree (and are non-eclipsing/ellipsoidal) is only 7, and the median mass is 0.82 $M_\odot$.

The classes of objects where the mass estimates agree best and most are the BLH and ACs. For these classes the estimates also agree with previous estimates in the literature. For the WVir the situation is slightly less clear but the mass estimates are similar to those of the BLH. The most confusing picture is presented by the pWVir and the RVT. The mass estimate for the former classes is definitely larger than for the BLH and WVir.

Some of the known binaries have a (spurious) large mass assigned: LMC -098 (3 $M_\odot$, pWVir), SMC -007 (1.9 $M_\odot$, RVT), -010 (2.3 $M_\odot$, pWVir), -028 (1.6 $M_\odot$, pWVir), and -029 (2.5 $M_\odot$, RVT). Based on this, the following stars (non ACs) could also be binaries: The LMC objects -032 (RVT, 1.9 $M_\odot$), -123 (BLHer, 2.2 $M_\odot$), -136 (BLHer, 2.0 $M_\odot$), -153 (BLHer, 1.6 $M_\odot$), -185 (WVir, 4.5 $M_\odot$), and SMC objects -001 (pWVir, 1.7 $M_\odot$), and -011 (pWVir, 1.8 $M_\odot$). The first 5 stars listed were also removed as outliers in the *PR* relation, and -153 and -185 were also removed as outliers in the $P - M_{\rm bol}$ relation. -185 was an outlier in the amplitude-magnitude diagram (Fig. 10 in GJ17). None of these stars were marked as possible binaries based on the LTT effect in GJ17 however. -153 has been indicated by the OGLE team as blended, and the finding chart for -156 on the OGLE-III Variable Stars Database (http://ogledb.astrouw.edu.pl/~ogle/CVS/) suggests it is blended as well, so for those stars that could easily be the cause of their brighter appearance. On the other hand, based on the mass estimate, period, and the fact that it is brighter and larger than the other BLH, -123 could be classified as an FU AC.

During the refereeing process Pilecki et al. (2017) appeared that analysed this system in detail and derived a mass of 1.51 ± 0.09 $M_\odot$, $T_{\rm eff}$ = 5300 ± 100 K, and L = 450 ± 40 $L_\odot$ for the pulsating star, and 6.8 ± 0.4 $M_\odot$, $T_{\rm eff}$ = 9500 ± 500 K, and $L = 5000 \pm 1100\, L_\odot$ for the secondary. Fitting the SED as a single object GJ17 found $T_{\rm eff}$ = 7375 ± 312 K and L = 2857 ± 169 $L_\odot$. Using the luminosity and effective temperature (and errors) from Pilecki et al. (2017) the mass estimate based on the Cepheid, respectively, RRL pulsation models is 1.37 ± 0.04 $M_\odot$, respectively, 1.52 ± 0.07 $M_\odot$, in agreement with Pilecki et al. (2017). The parameters they derived, in particular the mass, depend on the adopted, so-called, projection factor, p. We find that the geometric mean of the Cepheid and RRL pulsation mass, and their derived mass agrees best for $p = 1.32 \pm 0.03$, in excellent agreement with their adopted $p = 1.30 \pm 0.04$. Interestingly, their derived values of $M_{\rm bol} = -1.88 \pm 0.09$ and $R = 25.2 \pm 0.4\ R_\odot$ (and that do not depend very much on the adopted value of p) still make the Cepheid overluminous and oversized with re-

spect to our preferred solutions of Tables 1 and 2 that give $M_{\rm bol} = -1.12 \pm 0.05$, and $R = 16.2 \pm 0.3\ R_{\odot}$.

The mass estimates for the RVT show both very large and very small values. As indicated above, many RVT have mass estimates that are well above that expected for a post-AGB object (0.55 - 1.1 $M_{\odot}$). In addition, of the about 30 stars that have a mass estimate below 0.35 $M_{\odot}$, 10 are RVT and 6 of those have a dust excess. Such low masses are also not expected from single-star evolution and, as remarked in in GJ17, the shape of the dust excess in these SEDs points to a disk-like structure that is thought to result from binary evolution. Possibly some are related to the so called binary evolutionary pulsators (BEP), binary stars that appear in the IS after significant mass transfer. Recently, Karczmarek et al. (2017) did extensive simulations to find contaminations of genuine RRL and classical Cepheids of respectively, 0.8 and 5% by BEP. In GJ17 we estimated that a contamination of several percent is plausible for T2C as well.

5. Summary and conclusions

The luminosities and effective temperatures derived in GJ17 for 335 T2Cs and ACs in the SMC and LMC were used to study the period-Wesenheit, and for the first time to our knowledge in the 21st Century, the period-bolometric luminosity and *PR* relations for these classes of stars.

The $P - M_{\rm bol}$ relation shows more scatter than the *PW* relation. This is likely due to the fact that the fits to the SEDs presented in GJ17 are based on non-contemporaneous photometry over a large wavelength region. This will introduce some "natural scatter", but will likely reveal the effect of binarity or blending more easily than when using only the OGLE mean *V*, *I* magnitudes. The period-bolometric luminosity and *PR* relations do not significantly depend on metallicity (as probed by the T2C in the SMC and LMC, and supported by the limited data for Galactic T2Cs), and excluding the dusty RVTs, the T2C can be described by single relationships.

We used the published results of theoretical pulsation models for classical Cepheids and RRL to derive period-luminosity-mass-temperature-metallicity relations. Assuming a metallicity these relations allow us to derive the pulsation mass for all objects based on both types of models. The RRL and CC models agree well and most for the BLH and ACs. The masses agree with those in the literature, respectively, $\sim 0.5\ M_{\odot}$ and $\sim 1.3\ M_{\odot}$. For the RVT the agreement with the two mass estimates is poorest, and often indicates masses that are inconsistent with single-star evolution of a post-AGB star: either above $\sim 1\ M_{\odot}$ or well below $\sim 0.5\ M_{\odot}$.

Acknowledgements. M.I.J. acknowledges financial support from the Ministry of Education, Science and Technological Development of the Republic of Serbia through the project 176004, and the Hungarian National Research, Development and Innovation Office through NKFIH K-115709. This research has made use of the VizieR catalogue access tool, CDS, Strasbourg, France. The original description of the VizieR service was published in A&AS 143, 23.

References

Balog, Z., Vinko, J., & Kaszas, G. 1997, AJ, 113, 1833
Benedict, G. F., McArthur, B. E., Feast, M. W., et al. 2011, AJ, 142, 187
Berdnikov, L. N. 2008, VizieR Online Data Catalog, 2285, 0
Bhardwaj, A., Macri, L. M., Rejkuba, M., et al. 2017, AJ, 153, 154
Bono, G., Caputo, F., & Marconi, M. 1998, ApJ, 497, L43
Bono, G., Caputo, F., & Santolamazza, P. 1997a, A&A, 317, 171
Bono, G., Caputo, F., Santolamazza, P., Cassisi, S., & Piersimoni, A. 1997b, AJ, 113, 2209
Bono, G., Castellani, V., & Marconi, M. 2000, ApJ, 529, 293
Breitfelder, J., Kervella, P., Mérand, A., et al. 2015, A&A, 576, A64
Burki, G. & Meylan, G. 1986, A&A, 159, 261
Caputo, F., Castellani, V., Degl'Innocenti, S., Fiorentino, G., & Marconi, M. 2004, A&A, 424, 927
Catelan, M. & Smith, H. A. 2015, Pulsating Stars
Cioni, M.-R. L., Clementini, G., Girardi, L., et al. 2011, A&A, 527, A116
Clementini, G., Ripepi, V., Leccia, S., et al. 2016, A&A, 595, A133
Di Criscienzo, M., Caputo, F., Marconi, M., & Cassisi, S. 2007, A&A, 471, 893
Feast, M. W., Laney, C. D., Kinman, T. D., van Leeuwen, F., & Whitelock, P. A. 2008, MNRAS, 386, 2115
Fiorentino, G. & Monelli, M. 2012, A&A, 540, A102
Gaia Collaboration, Prusti, T., de Bruijne, J. H. J., et al. 2016, A&A, 595, A1
Gratton, R. G., Bragaglia, A., Clementini, G., et al. 2004, A&A, 421, 937
Groenewegen, M. A. T. 2012, A&A, 543, A36
Groenewegen, M. A. T. & Jurkovic, M. 2017, ArXiv e-prints [arXiv:1705.00886]
Groenewegen, M. A. T., Udalski, A., & Bono, G. 2008, A&A, 481, 441
Irwin, J. B. 1952, ApJ, 116, 211
Ivezić, Ž., Nenkova, M., & Elitzur, M. 1999, DUSTY: Radiation transport in a dusty environment, Astrophysics Source Code Library
Kamath, D., Wood, P. R., Van Winckel, H., & Nie, J. D. 2016, A&A, 586, L5
Karczmarek, P., Wiktorowicz, G., Iłkiewicz, K., et al. 2017, MNRAS, 466, 2842
Luck, R. E. & Bond, H. E. 1989, ApJ, 342, 476
Macri, L. M., Ngeow, C.-C., Kanbur, S. M., Mahzooni, S., & Smitka, M. T. 2015, AJ, 149, 117
Manick, R., Van Winckel, H., Kamath, D., Hillen, M., & Escorza, A. 2017, A&A, 597, A129
Marconi, M., Coppola, G., Bono, G., et al. 2015, ApJ, 808, 50
Marconi, M., Fiorentino, G., & Caputo, F. 2004, A&A, 417, 1101
Marconi, M., Molinaro, R., Bono, G., et al. 2013, ApJ, 768, L6
Martínez-Vázquez, C. E., Stetson, P. B., Monelli, M., et al. 2016, MNRAS, 462, 4349
Matsunaga, N., Feast, M. W., & Menzies, J. W. 2009, MNRAS, 397, 933
Matsunaga, N., Feast, M. W., & Soszyński, I. 2011, MNRAS, 413, 223
Matsunaga, N., Fukushi, H., Nakada, Y., et al. 2006, MNRAS, 370, 1979
Nemec, J. M., Nemec, A. F. L., & Lutz, T. E. 1994, AJ, 108, 222
Pilecki, B., Gieren, W., Smolec, R., et al. 2017, ArXiv e-prints [arXiv:1704.07782]
Pilecki, B., Graczyk, D., Pietrzyński, G., et al. 2013, MNRAS, 436, 953
Ripepi, V., Marconi, M., Moretti, M. I., et al. 2014, MNRAS, 437, 2307
Ripepi, V., Moretti, M. I., Marconi, M., et al. 2015, MNRAS, 446, 3034
Romaniello, M., Primas, F., Mottini, M., et al. 2008, A&A, 488, 731
Sandage, A. & Tammann, G. A. 2006, ARA&A, 44, 93
Soszyński, I., Poleski, R., Udalski, A., et al. 2008a, Acta Astron., 58, 163
Soszyński, I., Poleski, R., Udalski, A., et al. 2010a, Acta Astron., 60, 17
Soszynski, I., Udalski, A., Szymanski, M., et al. 2003, Acta Astron., 53, 93
Soszyński, I., Udalski, A., Szymański, M. K., et al. 2010b, Acta Astron., 60, 91
Soszyński, I., Udalski, A., Szymański, M. K., et al. 2008b, Acta Astron., 58, 293
Vassiliadis, E. & Wood, P. R. 1993, ApJ, 413, 641
Wallerstein, G. 2002, PASP, 114, 689

Appendix A: Mass estimates

Table A.1 contains the radii with error bars, and the mass estimates and error bars for individual object based on the Cepheid and RRL pulsation models (Eqs. 5 and 6). For reference it is also indicated if the star has an IR excess (Dusty=1), or is a known binary (Binary=1). If the two mass estimates agree within 3× the combined error bars the last column has an "OK" listed, and else, if the two mass estimates still agree within 15% (without considering the errors) the last column has an "ok" listed.

Table A.1. Mass estimates

Name	Type	Period (d)	Radius ($R_\odot$)	$\mathrm{Mass_{Cep}}$ ($M_\odot$)	$\mathrm{Mass_{RRL}}$ ($M_\odot$)	Dusty?	Binary?	Agree?
OGLE-LMC-ACEP-001	F	0.85	7.86 ± 0.48	0.891 ± 0.016	1.023 ± 0.029	0	0	ok
OGLE-LMC-ACEP-002	F	0.98	9.32 ± 0.56	1.127 ± 0.022	1.314 ± 0.045	0	0	ok
OGLE-LMC-ACEP-003	1O	0.51	5.94 ± 0.43	0.925 ± 0.020	1.063 ± 0.041	0	0	ok
OGLE-LMC-ACEP-004	F	1.86	13.12 ± 2.99	1.091 ± 0.202	1.202 ± 0.383	0	0	OK
OGLE-LMC-ACEP-005	F	0.93	8.53 ± 0.50	0.960 ± 0.017	1.106 ± 0.032	0	0	ok
OGLE-LMC-ACEP-006	1O	1.14	12.07 ± 0.71	1.703 ± 0.042	2.115 ± 0.110	0	0	
OGLE-LMC-ACEP-007	F	0.90	8.75 ± 0.66	1.096 ± 0.029	1.267 ± 0.064	0	0	OK
OGLE-LMC-ACEP-008	1O	1.00	10.64 ± 0.44	1.500 ± 0.020	1.820 ± 0.043	0	0	
OGLE-LMC-ACEP-009	1O	1.07	10.56 ± 0.42	1.344 ± 0.016	1.605 ± 0.032	0	0	
OGLE-LMC-ACEP-010	F	0.83	7.69 ± 0.73	0.878 ± 0.029	0.993 ± 0.059	0	0	OK
OGLE-LMC-ACEP-011	F	1.00	11.44 ± 1.01	1.667 ± 0.085	2.253 ± 0.260	0	0	OK
OGLE-LMC-ACEP-012	F	0.83	9.99 ± 2.88	1.571 ± 0.619	2.083 ± 1.623	0	0	OK
OGLE-LMC-ACEP-013	1O	0.67	7.51 ± 1.08	1.090 ± 0.090	1.321 ± 0.218	0	0	OK
OGLE-LMC-ACEP-014	F	2.29	15.37 ± 0.63	1.233 ± 0.015	1.339 ± 0.025	0	0	ok
OGLE-LMC-ACEP-015	1O	1.58	12.12 ± 0.69	1.150 ± 0.020	1.252 ± 0.038	0	0	OK
OGLE-LMC-ACEP-016	F	1.55	12.51 ± 0.76	1.261 ± 0.026	1.422 ± 0.053	0	0	OK
OGLE-LMC-ACEP-017	F	0.93	9.64 ± 0.39	1.298 ± 0.016	1.565 ± 0.031	0	0	
OGLE-LMC-ACEP-018	F	1.02	8.80 ± 0.80	0.957 ± 0.031	1.046 ± 0.061	0	0	OK
OGLE-LMC-ACEP-019	F	0.91	9.23 ± 0.50	1.259 ± 0.022	1.435 ± 0.045	0	0	ok
OGLE-LMC-ACEP-020	1O	0.51	6.14 ± 0.50	1.047 ± 0.031	1.161 ± 0.062	0	0	OK
OGLE-LMC-ACEP-021	F	1.30	11.22 ± 1.83	1.206 ± 0.136	1.396 ± 0.299	0	0	OK
OGLE-LMC-ACEP-023	1O	0.97	11.32 ± 0.69	1.811 ± 0.052	2.291 ± 0.137	0	0	
OGLE-LMC-ACEP-024	F	0.79	6.98 ± 0.24	0.825 ± 0.011	0.817 ± 0.012	0	0	OK
OGLE-LMC-ACEP-025	1O	0.64	6.82 ± 0.90	0.991 ± 0.064	1.097 ± 0.129	0	0	OK
OGLE-LMC-ACEP-026	F	1.74	14.61 ± 0.61	1.509 ± 0.020	1.815 ± 0.044	0	0	
OGLE-LMC-ACEP-027	F	1.27	11.76 ± 1.09	1.430 ± 0.069	1.649 ± 0.154	0	0	OK
OGLE-LMC-ACEP-028	1O	0.80	12.17 ± 1.33	2.467 ± 0.276	3.821 ± 1.117	0	0	OK
OGLE-LMC-ACEP-029	F	0.80	6.69 ± 0.48	0.688 ± 0.014	0.715 ± 0.021	0	0	OK
OGLE-LMC-ACEP-030	1O	0.89	10.40 ± 0.78	1.662 ± 0.063	2.060 ± 0.163	0	0	OK
OGLE-LMC-ACEP-031	1O	1.12	10.61 ± 1.34	1.293 ± 0.099	1.502 ± 0.223	0	0	OK
OGLE-LMC-ACEP-032	F	1.32	12.24 ± 0.52	1.432 ± 0.019	1.737 ± 0.041	0	0	
OGLE-LMC-ACEP-033	F	2.35	15.90 ± 0.66	1.278 ± 0.016	1.414 ± 0.027	0	0	ok
OGLE-LMC-ACEP-034	F	0.73	8.05 ± 1.75	1.156 ± 0.209	1.383 ± 0.469	0	0	OK
OGLE-LMC-ACEP-035	1O	0.60	6.64 ± 0.25	0.977 ± 0.012	1.129 ± 0.017	0	0	ok
OGLE-LMC-ACEP-036	F	1.26	12.09 ± 0.50	1.473 ± 0.019	1.807 ± 0.042	0	0	
OGLE-LMC-ACEP-037	F	1.26	20.42 ± 2.77	4.582 ± 1.417	7.854 ± 6.898	0	0	OK
OGLE-LMC-ACEP-038	F	1.34	10.51 ± 0.61	1.019 ± 0.017	1.107 ± 0.031	0	0	OK
OGLE-LMC-ACEP-039	F	0.99	8.81 ± 0.18	0.981 ± 0.010	1.095 ± 0.011	0	0	ok
OGLE-LMC-ACEP-040	F	0.96	10.81 ± 1.25	1.589 ± 0.128	2.044 ± 0.356	0	0	OK
OGLE-LMC-ACEP-041	F	0.88	8.57 ± 1.64	1.058 ± 0.141	1.235 ± 0.306	0	0	OK
OGLE-LMC-ACEP-042	F	1.08	12.10 ± 0.63	1.613 ± 0.032	2.329 ± 0.105	0	0	
OGLE-LMC-ACEP-043	1O	0.68	8.53 ± 0.35	1.414 ± 0.018	1.854 ± 0.044	0	0	
OGLE-LMC-ACEP-044	F	1.31	11.09 ± 0.99	1.224 ± 0.048	1.327 ± 0.094	0	0	OK
OGLE-LMC-ACEP-045	F	0.68	6.83 ± 0.53	0.851 ± 0.020	0.994 ± 0.042	0	0	ok
OGLE-LMC-ACEP-046	F	1.26	11.00 ± 1.58	1.214 ± 0.110	1.374 ± 0.233	0	0	OK
OGLE-LMC-ACEP-047	F	2.18	12.63 ± 0.74	0.849 ± 0.014	0.838 ± 0.020	0	0	OK
OGLE-LMC-ACEP-048	F	1.55	14.07 ± 1.88	1.622 ± 0.173	1.978 ± 0.428	0	0	OK
OGLE-LMC-ACEP-049	F	0.64	6.67 ± 0.99	0.915 ± 0.068	1.008 ± 0.134	0	0	OK
OGLE-LMC-ACEP-050	1O	1.40	13.40 ± 0.51	1.750 ± 0.023	2.022 ± 0.046	0	0	ok
OGLE-LMC-ACEP-051	F	0.71	7.32 ± 0.15	0.949 ± 0.010	1.128 ± 0.011	0	0	
OGLE-LMC-ACEP-052	F	1.26	12.30 ± 1.20	1.544 ± 0.088	1.885 ± 0.222	0	0	OK
OGLE-LMC-ACEP-053	F	1.89	16.49 ± 1.99	1.785 ± 0.174	2.231 ± 0.456	0	0	OK
OGLE-LMC-ACEP-054	F	0.98	10.45 ± 0.70	1.346 ± 0.035	1.804 ± 0.103	0	0	
OGLE-LMC-ACEP-055	F	1.61	13.24 ± 1.58	1.326 ± 0.094	1.569 ± 0.220	0	0	OK
OGLE-LMC-ACEP-056	F	1.12	10.68 ± 1.57	1.284 ± 0.129	1.532 ± 0.304	0	0	OK
OGLE-LMC-ACEP-057	F	1.71	14.65 ± 0.89	1.572 ± 0.039	1.882 ± 0.094	0	0	
OGLE-LMC-ACEP-058	1O	0.65	6.40 ± 1.16	0.889 ± 0.090	0.885 ± 0.143	0	0	OK
OGLE-LMC-ACEP-059	F	0.83	10.67 ± 0.86	1.564 ± 0.064	2.490 ± 0.274	0	0	
OGLE-LMC-ACEP-060	F	1.28	12.21 ± 0.91	1.532 ± 0.053	1.814 ± 0.127	0	0	OK

Table A.1. Continued

Name	Type	Period (d)	Radius ($R_\odot$)	Mass_{Cep} ($M_\odot$)	Mass_{RRL} ($M_\odot$)	Dusty?	Binary?	Agree?
OGLE-LMC-ACEP-061	F	0.85	8.84 ± 0.52	1.175 ± 0.022	1.425 ± 0.052	0	0	
OGLE-LMC-ACEP-062	F	1.06	10.02 ± 1.33	1.284 ± 0.107	1.407 ± 0.213	0	0	OK
OGLE-LMC-ACEP-063	F	0.89	8.86 ± 0.75	1.055 ± 0.033	1.320 ± 0.085	0	0	OK
OGLE-LMC-ACEP-064	F	1.36	12.17 ± 0.93	1.392 ± 0.046	1.627 ± 0.106	0	0	OK
OGLE-LMC-ACEP-065	F	1.32	11.03 ± 1.38	1.169 ± 0.080	1.289 ± 0.161	0	0	OK
OGLE-LMC-ACEP-066	F	1.04	9.50 ± 0.72	1.089 ± 0.029	1.252 ± 0.063	0	0	OK
OGLE-LMC-ACEP-067	F	0.82	10.16 ± 3.10	1.635 ± 0.735	2.221 ± 2.000	0	0	OK
OGLE-LMC-ACEP-068	F	0.63	5.68 ± 0.85	0.652 ± 0.036	0.674 ± 0.061	0	0	OK
OGLE-LMC-ACEP-069	F	1.54	15.40 ± 1.25	1.991 ± 0.104	2.567 ± 0.295	0	0	OK
OGLE-LMC-ACEP-070	1O	0.84	7.82 ± 0.71	0.918 ± 0.029	1.019 ± 0.058	0	0	OK
OGLE-LMC-ACEP-071	1O	0.91	8.59 ± 0.88	1.102 ± 0.049	1.180 ± 0.094	0	0	OK
OGLE-LMC-ACEP-072	F	1.05	11.21 ± 1.21	1.622 ± 0.117	1.961 ± 0.289	0	0	OK
OGLE-LMC-ACEP-073	F	1.47	13.12 ± 1.65	1.523 ± 0.137	1.770 ± 0.310	0	0	OK
OGLE-LMC-ACEP-074	F	1.53	12.69 ± 0.74	1.317 ± 0.026	1.500 ± 0.055	0	0	ok
OGLE-LMC-ACEP-075	F	0.69	7.40 ± 0.67	1.034 ± 0.036	1.203 ± 0.080	0	0	OK
OGLE-LMC-ACEP-076	F	1.58	11.87 ± 1.11	1.083 ± 0.041	1.182 ± 0.082	0	0	OK
OGLE-LMC-ACEP-077	F	1.12	10.98 ± 0.50	1.342 ± 0.019	1.662 ± 0.043	0	0	
OGLE-LMC-ACEP-078	1O	1.15	10.84 ± 0.58	1.383 ± 0.025	1.542 ± 0.050	0	0	OK
OGLE-LMC-ACEP-079	F	1.16	10.80 ± 0.82	1.330 ± 0.042	1.509 ± 0.089	0	0	OK
OGLE-LMC-ACEP-080	F	1.06	9.83 ± 0.74	1.169 ± 0.032	1.342 ± 0.070	0	0	OK
OGLE-LMC-ACEP-081	F	0.80	7.75 ± 0.45	0.949 ± 0.016	1.081 ± 0.030	0	0	ok
OGLE-LMC-ACEP-082	1O	1.04	13.07 ± 0.58	2.166 ± 0.041	3.070 ± 0.137	0	0	
OGLE-LMC-T2CEP-001	BLHer	1.81	9.31 ± 0.20	0.507 ± 0.010	0.481 ± 0.010	0	0	OK
OGLE-LMC-T2CEP-002	WVir	18.32	30.37 ± 3.39	0.411 ± 0.013	0.310 ± 0.013	0	0	
OGLE-LMC-T2CEP-003	RVTau	35.66	60.28 ± 8.03	0.953 ± 0.060	0.714 ± 0.056	1	0	OK
OGLE-LMC-T2CEP-004	BLHer	1.92	12.62 ± 1.84	0.928 ± 0.066	1.032 ± 0.134	0	0	OK
OGLE-LMC-T2CEP-005	RVTau	33.19	50.18 ± 6.41	0.605 ± 0.024	0.483 ± 0.025	0	0	
OGLE-LMC-T2CEP-006	BLHer	1.09	6.26 ± 0.54	0.414 ± 0.011	0.361 ± 0.012	0	0	ok
OGLE-LMC-T2CEP-007	BLHer	1.24	6.82 ± 0.49	0.421 ± 0.011	0.372 ± 0.011	0	0	ok
OGLE-LMC-T2CEP-008	BLHer	1.75	9.19 ± 0.39	0.509 ± 0.010	0.493 ± 0.011	0	0	OK
OGLE-LMC-T2CEP-009	BLHer	1.76	8.71 ± 0.35	0.460 ± 0.010	0.418 ± 0.010	0	0	OK
OGLE-LMC-T2CEP-010	BLHer	1.50	7.35 ± 0.54	0.386 ± 0.011	0.336 ± 0.011	0	0	ok
OGLE-LMC-T2CEP-011	RVTau	39.26	52.01 ± 2.21	0.592 ± 0.010	0.405 ± 0.010	1	0	
OGLE-LMC-T2CEP-012	WVir	11.58	24.80 ± 2.23	0.454 ± 0.012	0.370 ± 0.012	0	0	
OGLE-LMC-T2CEP-013	WVir	11.54	23.84 ± 1.12	0.416 ± 0.010	0.333 ± 0.010	0	0	
OGLE-LMC-T2CEP-014	RVTau	61.88	48.67 ± 2.12	0.283 ± 0.010	0.161 ± 0.010	1	0	
OGLE-LMC-T2CEP-015	RVTau	56.52	72.01 ± 3.53	0.732 ± 0.011	0.559 ± 0.011	1	0	
OGLE-LMC-T2CEP-016	RVTau	20.30	23.45 ± 2.12	0.228 ± 0.010	0.127 ± 0.010	1	0	
OGLE-LMC-T2CEP-017	WVir	14.45	30.64 ± 2.31	0.541 ± 0.012	0.467 ± 0.013	0	0	
OGLE-LMC-T2CEP-018	BLHer	1.38	7.70 ± 0.30	0.474 ± 0.010	0.440 ± 0.010	0	0	OK
OGLE-LMC-T2CEP-019	pWVir	8.67	27.86 ± 6.88	0.833 ± 0.135	0.819 ± 0.201	0	0	OK
OGLE-LMC-T2CEP-020	BLHer	1.11	7.60 ± 0.70	0.611 ± 0.016	0.605 ± 0.023	0	0	OK
OGLE-LMC-T2CEP-021	pWVir	9.76	23.72 ± 1.04	0.534 ± 0.010	0.430 ± 0.010	0	1	
OGLE-LMC-T2CEP-022	WVir	10.72	23.70 ± 1.62	0.450 ± 0.011	0.369 ± 0.011	0	0	
OGLE-LMC-T2CEP-023	pWVir	5.23	24.72 ± 1.90	1.343 ± 0.044	1.323 ± 0.072	0	1	OK
OGLE-LMC-T2CEP-024	BLHer	1.25	6.85 ± 0.74	0.413 ± 0.012	0.373 ± 0.014	0	0	OK
OGLE-LMC-T2CEP-025	RVTau	67.97	75.77 ± 9.15	0.645 ± 0.025	0.478 ± 0.023	0	0	
OGLE-LMC-T2CEP-026	WVir	13.58	28.09 ± 1.39	0.485 ± 0.010	0.406 ± 0.010	0	0	
OGLE-LMC-T2CEP-027	WVir	17.13	27.46 ± 3.44	0.362 ± 0.013	0.260 ± 0.012	0	0	
OGLE-LMC-T2CEP-028	pWVir	8.78	23.71 ± 2.61	0.645 ± 0.022	0.508 ± 0.022	0	0	
OGLE-LMC-T2CEP-029	RVTau	31.25	53.89 ± 3.43	0.845 ± 0.015	0.648 ± 0.016	1	0	
OGLE-LMC-T2CEP-030	BLHer	3.94	14.34 ± 0.63	0.514 ± 0.010	0.459 ± 0.010	0	0	ok
OGLE-LMC-T2CEP-031	WVir	6.71	18.38 ± 0.84	0.454 ± 0.010	0.388 ± 0.010	0	0	
OGLE-LMC-T2CEP-032	RVTau	44.56	96.44 ± 32.06	1.865 ± 1.092	1.863 ± 1.571	1	0	OK
OGLE-LMC-T2CEP-033	pWVir	9.39	23.79 ± 1.92	0.571 ± 0.013	0.461 ± 0.014	0	0	
OGLE-LMC-T2CEP-034	WVir	14.91	29.99 ± 1.60	0.488 ± 0.010	0.419 ± 0.011	0	0	
OGLE-LMC-T2CEP-035	WVir	9.87	26.15 ± 2.49	0.612 ± 0.017	0.557 ± 0.021	0	0	OK

Table A.1. Continued

Name	Type	Period (d)	Radius ($R_\odot$)	$\mathrm{Mass_{Cep}}$ ($M_\odot$)	$\mathrm{Mass_{RRL}}$ ($M_\odot$)	Dusty?	Binary?	Agree?
OGLE-LMC-T2CEP-036	WVir	14.88	23.60 ± 1.55	0.308 ± 0.010	0.214 ± 0.010	0	0	
OGLE-LMC-T2CEP-037	WVir	6.90	17.20 ± 0.75	0.385 ± 0.010	0.308 ± 0.010	0	0	
OGLE-LMC-T2CEP-038	WVir	4.01	14.72 ± 1.46	0.607 ± 0.017	0.476 ± 0.018	0	0	
OGLE-LMC-T2CEP-039	WVir	8.72	20.20 ± 1.72	0.418 ± 0.011	0.330 ± 0.011	0	0	
OGLE-LMC-T2CEP-040	pWVir	9.63	33.74 ± 4.61	1.143 ± 0.090	1.182 ± 0.159	0	0	OK
OGLE-LMC-T2CEP-041	BLHer	2.48	10.81 ± 1.53	0.541 ± 0.023	0.440 ± 0.025	0	0	OK
OGLE-LMC-T2CEP-042	pWVir	4.92	14.36 ± 2.17	0.427 ± 0.018	0.320 ± 0.017	0	0	
OGLE-LMC-T2CEP-043	WVir	6.56	16.79 ± 1.13	0.378 ± 0.010	0.312 ± 0.010	0	0	
OGLE-LMC-T2CEP-044	WVir	13.27	25.38 ± 1.74	0.405 ± 0.010	0.316 ± 0.011	0	0	
OGLE-LMC-T2CEP-045	RVTau	63.39	74.94 ± 3.79	0.706 ± 0.011	0.519 ± 0.011	0	0	
OGLE-LMC-T2CEP-046	WVir	14.74	35.90 ± 1.70	0.797 ± 0.012	0.704 ± 0.013	1	0	ok
OGLE-LMC-T2CEP-047	WVir	7.29	18.63 ± 1.60	0.427 ± 0.011	0.352 ± 0.012	0	0	
OGLE-LMC-T2CEP-048	BLHer	1.45	7.89 ± 1.71	0.473 ± 0.036	0.436 ± 0.048	0	0	OK
OGLE-LMC-T2CEP-049	BLHer	3.24	12.47 ± 2.71	0.503 ± 0.041	0.426 ± 0.045	0	0	OK
OGLE-LMC-T2CEP-050	RVTau	34.75	36.52 ± 1.57	0.302 ± 0.010	0.184 ± 0.010	1	0	
OGLE-LMC-T2CEP-051	RVTau	40.61	47.45 ± 3.14	0.441 ± 0.011	0.297 ± 0.010	0	0	
OGLE-LMC-T2CEP-052	pWVir	4.69	14.41 ± 1.91	0.466 ± 0.017	0.349 ± 0.016	0	1	
OGLE-LMC-T2CEP-053	BLHer	1.04	6.84 ± 0.38	0.520 ± 0.011	0.496 ± 0.011	0	0	OK
OGLE-LMC-T2CEP-054	WVir	9.93	23.35 ± 0.57	0.473 ± 0.010	0.401 ± 0.010	0	0	
OGLE-LMC-T2CEP-055	RVTau	41.01	50.93 ± 3.26	0.527 ± 0.011	0.356 ± 0.011	1	0	
OGLE-LMC-T2CEP-056	WVir	7.29	19.92 ± 0.49	0.480 ± 0.010	0.425 ± 0.010	0	0	ok
OGLE-LMC-T2CEP-057	WVir	16.63	30.31 ± 3.42	0.456 ± 0.014	0.361 ± 0.015	0	0	
OGLE-LMC-T2CEP-058	RVTau	21.48	33.97 ± 3.83	0.431 ± 0.013	0.328 ± 0.013	0	0	
OGLE-LMC-T2CEP-059	WVir	16.74	34.09 ± 3.16	0.595 ± 0.015	0.496 ± 0.017	0	0	
OGLE-LMC-T2CEP-060	BLHer	1.24	7.30 ± 1.39	0.474 ± 0.030	0.453 ± 0.042	0	0	OK
OGLE-LMC-T2CEP-061	BLHer	1.18	5.96 ± 0.86	0.336 ± 0.013	0.275 ± 0.014	0	0	
OGLE-LMC-T2CEP-062	WVir	6.05	20.36 ± 3.43	0.612 ± 0.039	0.612 ± 0.061	0	0	OK
OGLE-LMC-T2CEP-063	WVir	6.92	17.59 ± 1.49	0.403 ± 0.011	0.325 ± 0.011	0	0	
OGLE-LMC-T2CEP-064	BLHer	2.13	9.80 ± 2.05	0.473 ± 0.034	0.429 ± 0.044	0	0	OK
OGLE-LMC-T2CEP-065	RVTau	35.05	45.67 ± 2.07	0.479 ± 0.010	0.339 ± 0.010	1	0	
OGLE-LMC-T2CEP-066	WVir	13.11	25.80 ± 0.64	0.421 ± 0.010	0.338 ± 0.010	0	0	
OGLE-LMC-T2CEP-067	RVTau	48.23	71.33 ± 10.49	0.978 ± 0.075	0.701 ± 0.064	1	0	OK
OGLE-LMC-T2CEP-068	BLHer	1.61	8.14 ± 0.60	0.449 ± 0.011	0.400 ± 0.012	0	0	ok
OGLE-LMC-T2CEP-069	BLHer	1.02	7.34 ± 1.96	0.630 ± 0.088	0.626 ± 0.130	0	0	OK
OGLE-LMC-T2CEP-070	WVir	15.44	25.12 ± 2.56	0.348 ± 0.011	0.240 ± 0.011	0	0	
OGLE-LMC-T2CEP-071	BLHer	1.15	7.14 ± 1.67	0.497 ± 0.045	0.476 ± 0.063	0	0	OK
OGLE-LMC-T2CEP-072	WVir	14.51	26.70 ± 1.23	0.412 ± 0.010	0.315 ± 0.010	0	0	
OGLE-LMC-T2CEP-073	BLHer	3.09	12.58 ± 1.02	0.519 ± 0.012	0.471 ± 0.014	0	0	OK
OGLE-LMC-T2CEP-074	WVir	8.99	22.53 ± 1.45	0.519 ± 0.011	0.426 ± 0.011	0	0	
OGLE-LMC-T2CEP-075	RVTau	50.19	54.91 ± 2.77	0.458 ± 0.010	0.317 ± 0.010	1	0	
OGLE-LMC-T2CEP-076	BLHer	2.10	10.40 ± 1.10	0.519 ± 0.015	0.516 ± 0.022	0	0	OK
OGLE-LMC-T2CEP-077	BLHer	1.21	6.82 ± 0.65	0.460 ± 0.012	0.385 ± 0.013	0	1	
OGLE-LMC-T2CEP-078	pWVir	6.72	28.22 ± 1.48	1.165 ± 0.019	1.285 ± 0.034	0	0	ok
OGLE-LMC-T2CEP-079	WVir	14.85	26.06 ± 2.02	0.359 ± 0.010	0.285 ± 0.011	0	0	
OGLE-LMC-T2CEP-080	RVTau	40.92	51.62 ± 4.44	0.539 ± 0.013	0.371 ± 0.012	1	0	
OGLE-LMC-T2CEP-081	WVir	9.48	22.20 ± 1.02	0.457 ± 0.010	0.375 ± 0.010	0	0	
OGLE-LMC-T2CEP-082	RVTau	35.12	42.65 ± 4.96	0.397 ± 0.013	0.279 ± 0.012	0	0	
OGLE-LMC-T2CEP-083	pWVir	5.97	17.78 ± 0.79	0.498 ± 0.010	0.427 ± 0.010	0	0	
OGLE-LMC-T2CEP-084	BLHer	1.77	8.96 ± 2.84	0.551 ± 0.089	0.447 ± 0.085	0	1	OK
OGLE-LMC-T2CEP-085	BLHer	3.41	11.36 ± 1.27	0.375 ± 0.012	0.302 ± 0.012	0	0	
OGLE-LMC-T2CEP-086	WVir	15.85	28.45 ± 1.87	0.434 ± 0.011	0.326 ± 0.011	0	0	
OGLE-LMC-T2CEP-087	WVir	5.18	16.11 ± 2.31	0.466 ± 0.019	0.407 ± 0.023	0	0	OK
OGLE-LMC-T2CEP-088	BLHer	1.95	7.79 ± 0.71	0.358 ± 0.011	0.258 ± 0.011	0	0	
OGLE-LMC-T2CEP-089	BLHer	1.17	6.87 ± 0.37	0.462 ± 0.010	0.419 ± 0.011	0	0	OK
OGLE-LMC-T2CEP-090	BLHer	1.48	8.38 ± 0.64	0.524 ± 0.012	0.499 ± 0.014	0	0	OK

Table A.1. Continued

Name	Type	Period (d)	Radius ($R_\odot$)	Mass_{Cep} ($M_\odot$)	Mass_{RRL} ($M_\odot$)	Dusty?	Binary?	Agree?
OGLE-LMC-T2CEP-091	RVTau	35.75	47.36 ± 8.04	0.572 ± 0.034	0.362 ± 0.024	1	0	
OGLE-LMC-T2CEP-092	BLHer	2.62	10.68 ± 1.94	0.441 ± 0.024	0.390 ± 0.030	0	0	OK
OGLE-LMC-T2CEP-093	WVir	17.59	33.65 ± 2.77	0.585 ± 0.014	0.440 ± 0.013	0	1	
OGLE-LMC-T2CEP-094	WVir	8.47	22.54 ± 1.13	0.524 ± 0.010	0.471 ± 0.011	0	0	ok
OGLE-LMC-T2CEP-095	WVir	5.00	15.79 ± 0.38	0.460 ± 0.010	0.408 ± 0.010	0	0	ok
OGLE-LMC-T2CEP-096	WVir	13.93	25.78 ± 2.78	0.400 ± 0.012	0.306 ± 0.012	0	0	
OGLE-LMC-T2CEP-097	WVir	10.51	22.69 ± 1.95	0.428 ± 0.011	0.338 ± 0.011	0	0	
OGLE-LMC-T2CEP-098	pWVir	4.97	32.80 ± 2.78	3.038 ± 0.263	3.159 ± 0.478	0	1	OK
OGLE-LMC-T2CEP-099	WVir	15.49	35.43 ± 2.77	0.677 ± 0.015	0.628 ± 0.019	0	0	OK
OGLE-LMC-T2CEP-100	WVir	7.43	15.73 ± 0.97	0.292 ± 0.010	0.212 ± 0.010	0	0	
OGLE-LMC-T2CEP-101	WVir	11.42	21.60 ± 2.54	0.357 ± 0.012	0.257 ± 0.012	0	0	
OGLE-LMC-T2CEP-102	BLHer	1.27	7.57 ± 0.90	0.528 ± 0.018	0.481 ± 0.023	0	0	OK
OGLE-LMC-T2CEP-103	WVir	12.91	24.61 ± 2.16	0.395 ± 0.011	0.304 ± 0.011	0	0	
OGLE-LMC-T2CEP-104	RVTau	24.88	47.95 ± 6.84	0.835 ± 0.052	0.676 ± 0.057	1	0	OK
OGLE-LMC-T2CEP-105	BLHer	1.49	8.54 ± 1.45	0.555 ± 0.033	0.520 ± 0.046	0	0	OK
OGLE-LMC-T2CEP-106	WVir	6.71	18.21 ± 1.20	0.450 ± 0.011	0.378 ± 0.011	0	0	
OGLE-LMC-T2CEP-107	BLHer	1.21	9.91 ± 1.67	0.962 ± 0.093	1.106 ± 0.200	0	0	OK
OGLE-LMC-T2CEP-108	RVTau	30.01	41.06 ± 1.79	0.471 ± 0.010	0.323 ± 0.010	0	0	
OGLE-LMC-T2CEP-109	BLHer	1.41	8.23 ± 0.50	0.420 ± 0.010	0.513 ± 0.012	0	0	
OGLE-LMC-T2CEP-110	WVir	7.08	18.84 ± 1.70	0.443 ± 0.012	0.381 ± 0.013	0	0	
OGLE-LMC-T2CEP-111	WVir	7.50	18.76 ± 0.84	0.419 ± 0.010	0.343 ± 0.010	0	0	
OGLE-LMC-T2CEP-112	RVTau	39.40	52.33 ± 3.32	0.605 ± 0.012	0.409 ± 0.011	1	0	
OGLE-LMC-T2CEP-113	BLHer	3.09	12.43 ± 2.30	0.540 ± 0.036	0.455 ± 0.040	0	0	OK
OGLE-LMC-T2CEP-114	F	1.09	10.01 ± 0.69	1.051 ± 0.023	1.345 ± 0.060	0	0	
OGLE-LMC-T2CEP-115	RVTau	24.97	37.00 ± 2.71	0.430 ± 0.011	0.326 ± 0.011	0	0	
OGLE-LMC-T2CEP-116	BLHer	1.97	9.80 ± 1.04	0.491 ± 0.014	0.488 ± 0.020	0	0	OK
OGLE-LMC-T2CEP-117	WVir	6.63	17.74 ± 0.80	0.429 ± 0.010	0.358 ± 0.010	0	0	
OGLE-LMC-T2CEP-118	WVir	12.70	26.27 ± 1.86	0.457 ± 0.011	0.375 ± 0.011	0	0	
OGLE-LMC-T2CEP-119	RVTau	33.83	49.26 ± 8.80	0.650 ± 0.048	0.442 ± 0.036	1	0	
OGLE-LMC-T2CEP-120	WVir	4.56	15.01 ± 0.99	0.464 ± 0.011	0.412 ± 0.011	0	0	ok
OGLE-LMC-T2CEP-121	BLHer	2.06	9.87 ± 1.67	0.489 ± 0.026	0.461 ± 0.036	0	0	OK
OGLE-LMC-T2CEP-122	BLHer	1.54	8.00 ± 0.81	0.427 ± 0.012	0.411 ± 0.015	0	0	OK
OGLE-LMC-T2CEP-123	BLHer	1.00	12.26 ± 1.97	1.824 ± 0.305	2.722 ± 1.103	0	0	OK
OGLE-LMC-T2CEP-124	BLHer	1.73	8.44 ± 1.12	0.426 ± 0.015	0.393 ± 0.020	0	0	OK
OGLE-LMC-T2CEP-125	RVTau	33.03	44.16 ± 4.13	0.464 ± 0.012	0.340 ± 0.012	0	0	
OGLE-LMC-T2CEP-126	WVir	16.33	31.95 ± 1.84	0.505 ± 0.011	0.432 ± 0.011	1	0	
OGLE-LMC-T2CEP-127	WVir	12.67	25.53 ± 4.32	0.446 ± 0.022	0.347 ± 0.022	1	0	
OGLE-LMC-T2CEP-128	WVir	18.49	36.69 ± 3.43	0.623 ± 0.017	0.519 ± 0.018	0	0	
OGLE-LMC-T2CEP-129	RVTau	62.51	51.88 ± 2.20	0.333 ± 0.010	0.189 ± 0.010	1	0	
OGLE-LMC-T2CEP-130	BLHer	1.94	9.09 ± 1.71	0.455 ± 0.027	0.402 ± 0.033	0	0	OK
OGLE-LMC-T2CEP-131	BLHer	1.41	7.49 ± 0.31	0.416 ± 0.010	0.391 ± 0.010	0	0	OK
OGLE-LMC-T2CEP-132	pWVir	10.02	24.52 ± 2.54	0.552 ± 0.016	0.453 ± 0.017	0	0	
OGLE-LMC-T2CEP-133	WVir	6.28	16.55 ± 1.37	0.400 ± 0.011	0.321 ± 0.011	0	0	
OGLE-LMC-T2CEP-134	pWVir	4.08	17.91 ± 1.39	0.857 ± 0.020	0.807 ± 0.029	0	0	OK
OGLE-LMC-T2CEP-135	RVTau	26.52	43.20 ± 3.11	0.573 ± 0.012	0.457 ± 0.012	0	0	
OGLE-LMC-T2CEP-136	BLHer	1.32	13.48 ± 4.37	1.719 ± 0.895	2.260 ± 2.246	0	0	OK
OGLE-LMC-T2CEP-137	WVir	6.36	17.18 ± 2.10	0.425 ± 0.014	0.350 ± 0.015	0	0	
OGLE-LMC-T2CEP-138	BLHer	1.39	10.25 ± 3.71	0.830 ± 0.247	0.968 ± 0.475	0	0	OK
OGLE-LMC-T2CEP-139	WVir	14.78	29.36 ± 1.46	0.483 ± 0.010	0.400 ± 0.010	0	0	
OGLE-LMC-T2CEP-140	BLHer	1.84	9.43 ± 0.92	0.512 ± 0.014	0.486 ± 0.018	0	0	OK
OGLE-LMC-T2CEP-141	BLHer	1.82	8.24 ± 1.12	0.374 ± 0.014	0.339 ± 0.016	0	0	OK
OGLE-LMC-T2CEP-142	BLHer	1.76	11.48 ± 0.27	0.817 ± 0.010	0.909 ± 0.011	0	0	ok
OGLE-LMC-T2CEP-143	WVir	14.57	23.64 ± 2.40	0.321 ± 0.011	0.223 ± 0.011	0	0	
OGLE-LMC-T2CEP-144	BLHer	1.94	11.73 ± 4.38	0.752 ± 0.209	0.826 ± 0.352	0	0	OK
OGLE-LMC-T2CEP-145	BLHer	3.34	12.91 ± 2.40	0.530 ± 0.035	0.446 ± 0.039	0	0	OK
OGLE-LMC-T2CEP-146	WVir	10.08	23.03 ± 1.69	0.443 ± 0.011	0.377 ± 0.011	0	0	
OGLE-LMC-T2CEP-147	RVTau	46.80	69.48 ± 6.46	0.977 ± 0.034	0.684 ± 0.029	1	0	
OGLE-LMC-T2CEP-148	BLHer	2.67	9.92 ± 0.76	0.370 ± 0.011	0.306 ± 0.011	0	0	
OGLE-LMC-T2CEP-149	RVTau	42.48	52.85 ± 4.45	0.550 ± 0.013	0.373 ± 0.012	0	0	

Table A.1. Continued

Name	Type	Period (d)	Radius ($R_\odot$)	$\mathrm{Mass_{Cep}}$ ($M_\odot$)	$\mathrm{Mass_{RRL}}$ ($M_\odot$)	Dusty?	Binary?	Agree?
OGLE-LMC-T2CEP-150	WVir	5.49	17.60 ± 0.67	0.585 ± 0.010	0.473 ± 0.010	1	0	
OGLE-LMC-T2CEP-151	WVir	7.89	19.46 ± 1.67	0.428 ± 0.011	0.350 ± 0.012	0	0	
OGLE-LMC-T2CEP-152	WVir	9.31	22.84 ± 2.52	0.493 ± 0.015	0.418 ± 0.017	0	0	
OGLE-LMC-T2CEP-153	BLHer	1.18	11.24 ± 0.71	1.591 ± 0.042	1.638 ± 0.075	0	0	OK
OGLE-LMC-T2CEP-154	pWVir	7.58	23.97 ± 0.92	0.822 ± 0.011	0.666 ± 0.011	0	0	
OGLE-LMC-T2CEP-155	WVir	6.90	22.43 ± 3.50	0.669 ± 0.040	0.647 ± 0.061	0	0	OK
OGLE-LMC-T2CEP-156	WVir	15.39	33.84 ± 3.31	0.631 ± 0.018	0.558 ± 0.021	1	0	OK
OGLE-LMC-T2CEP-157	WVir	14.33	27.71 ± 1.38	0.439 ± 0.010	0.358 ± 0.010	0	0	
OGLE-LMC-T2CEP-158	WVir	7.14	18.13 ± 1.22	0.412 ± 0.010	0.337 ± 0.011	1	0	
OGLE-LMC-T2CEP-159	WVir	6.63	18.90 ± 0.47	0.478 ± 0.010	0.428 ± 0.010	0	0	ok
OGLE-LMC-T2CEP-160	BLHer	1.76	9.15 ± 1.08	0.500 ± 0.016	0.482 ± 0.023	0	0	OK
OGLE-LMC-T2CEP-161	WVir	8.53	29.73 ± 3.39	1.004 ± 0.050	1.009 ± 0.085	0	0	OK
OGLE-LMC-T2CEP-162	RVTau	30.39	44.46 ± 3.27	0.516 ± 0.012	0.397 ± 0.012	1	0	
OGLE-LMC-T2CEP-163	BLHer	1.69	10.11 ± 2.40	0.684 ± 0.085	0.676 ± 0.128	0	0	OK
OGLE-LMC-T2CEP-164	pWVir	8.50	25.88 ± 2.23	0.759 ± 0.019	0.688 ± 0.026	1	0	OK
OGLE-LMC-T2CEP-165	BLHer	1.24	8.30 ± 0.43	0.554 ± 0.011	0.647 ± 0.013	0	0	ok
OGLE-LMC-T2CEP-166	BLHer	2.11	15.33 ± 1.59	1.293 ± 0.070	1.518 ± 0.162	0	0	OK
OGLE-LMC-T2CEP-167	BLHer	2.31	11.49 ± 1.68	0.574 ± 0.027	0.586 ± 0.045	0	0	OK
OGLE-LMC-T2CEP-168	WVir	15.70	28.51 ± 1.36	0.430 ± 0.010	0.334 ± 0.010	0	0	
OGLE-LMC-T2CEP-169	RVTau	30.96	37.17 ± 7.37	0.377 ± 0.021	0.232 ± 0.015	1	0	
OGLE-LMC-T2CEP-170	WVir	7.68	19.64 ± 0.49	0.435 ± 0.010	0.375 ± 0.010	0	0	
OGLE-LMC-T2CEP-171	BLHer	1.55	8.56 ± 1.35	0.523 ± 0.026	0.488 ± 0.036	0	0	OK
OGLE-LMC-T2CEP-172	WVir	11.22	25.68 ± 2.57	0.492 ± 0.014	0.430 ± 0.016	0	0	OK
OGLE-LMC-T2CEP-173	WVir	4.15	16.30 ± 0.99	0.523 ± 0.011	0.608 ± 0.014	0	0	ok
OGLE-LMC-T2CEP-174	RVTau	46.82	75.02 ± 10.04	1.129 ± 0.084	0.848 ± 0.079	1	0	OK
OGLE-LMC-T2CEP-175	WVir	9.33	22.04 ± 1.03	0.453 ± 0.010	0.378 ± 0.010	0	0	
OGLE-LMC-T2CEP-176	WVir	7.99	20.49 ± 0.93	0.470 ± 0.010	0.396 ± 0.010	0	0	
OGLE-LMC-T2CEP-177	WVir	15.04	28.00 ± 2.04	0.424 ± 0.011	0.341 ± 0.011	0	0	
OGLE-LMC-T2CEP-178	WVir	12.21	23.84 ± 1.74	0.378 ± 0.010	0.304 ± 0.011	0	0	
OGLE-LMC-T2CEP-179	WVir	8.05	20.25 ± 0.53	0.434 ± 0.010	0.379 ± 0.010	0	0	ok
OGLE-LMC-T2CEP-180	RVTau	31.00	61.81 ± 10.03	1.147 ± 0.123	0.964 ± 0.142	1	0	OK
OGLE-LMC-T2CEP-181	pWVir	7.21	23.87 ± 2.63	0.762 ± 0.029	0.716 ± 0.041	0	0	OK
OGLE-LMC-T2CEP-182	WVir	8.23	23.35 ± 1.11	0.606 ± 0.011	0.544 ± 0.011	0	0	ok
OGLE-LMC-T2CEP-183	WVir	6.51	18.78 ± 1.11	0.455 ± 0.010	0.434 ± 0.011	0	0	OK
OGLE-LMC-T2CEP-184	WVir	14.84	27.43 ± 2.21	0.393 ± 0.011	0.329 ± 0.011	0	0	
OGLE-LMC-T2CEP-185	WVir	12.69	66.95 ± 1.87	3.832 ± 0.057	5.143 ± 0.160	0	0	
OGLE-LMC-T2CEP-186	WVir	16.36	31.99 ± 1.66	0.513 ± 0.010	0.431 ± 0.011	0	0	
OGLE-LMC-T2CEP-187	BLHer	2.40	10.82 ± 1.36	0.482 ± 0.017	0.465 ± 0.023	0	0	OK
OGLE-LMC-T2CEP-188	BLHer	1.05	8.29 ± 0.95	0.775 ± 0.031	0.843 ± 0.060	0	0	OK
OGLE-LMC-T2CEP-189	BLHer	1.31	7.58 ± 0.30	0.483 ± 0.010	0.459 ± 0.010	0	0	OK
OGLE-LMC-T2CEP-190	RVTau	38.36	52.21 ± 3.37	0.600 ± 0.012	0.425 ± 0.011	1	0	
OGLE-LMC-T2CEP-191	RVTau	34.34	63.59 ± 5.29	1.105 ± 0.035	0.883 ± 0.038	1	0	
OGLE-LMC-T2CEP-192	RVTau	26.19	34.96 ± 3.10	0.370 ± 0.011	0.257 ± 0.011	0	0	
OGLE-LMC-T2CEP-193	WVir	7.00	20.00 ± 0.49	0.516 ± 0.010	0.458 ± 0.010	0	0	ok
OGLE-LMC-T2CEP-194	BLHer	1.31	8.25 ± 0.64	0.592 ± 0.013	0.578 ± 0.017	0	0	OK
OGLE-LMC-T2CEP-195	BLHer	2.75	11.49 ± 1.15	0.485 ± 0.013	0.441 ± 0.016	0	0	OK
OGLE-LMC-T2CEP-196	WVir	14.96	32.84 ± 2.33	0.627 ± 0.013	0.536 ± 0.014	0	0	
OGLE-LMC-T2CEP-197	BLHer	1.22	8.07 ± 1.04	0.613 ± 0.025	0.608 ± 0.039	0	0	OK
OGLE-LMC-T2CEP-198	RVTau	38.27	49.65 ± 2.79	0.472 ± 0.010	0.373 ± 0.010	0	0	
OGLE-LMC-T2CEP-199	RVTau	37.20	38.00 ± 2.67	0.377 ± 0.010	0.182 ± 0.010	1	0	
OGLE-LMC-T2CEP-200	RVTau	34.92	57.81 ± 8.19	0.790 ± 0.047	0.661 ± 0.053	1	0	OK
OGLE-LMC-T2CEP-201	pWVir	11.01	36.81 ± 2.77	1.372 ± 0.044	1.207 ± 0.057	1	0	OK
OGLE-LMC-T2CEP-202	RVTau	38.14	50.01 ± 2.66	0.490 ± 0.010	0.382 ± 0.010	0	0	
OGLE-LMC-T2CEP-203	RVTau	37.13	46.46 ± 3.67	0.427 ± 0.011	0.325 ± 0.011	0	0	

Table A.1. Continued

Name	Type	Period (d)	Radius ($R_\odot$)	Mass_{Cep} ($M_\odot$)	Mass_{RRL} ($M_\odot$)	Dusty?	Binary?	Agree?
OGLE-SMC-ACEP-01	1O	0.83	6.88 ± 0.36	0.738 ± 0.012	0.728 ± 0.014	0	0	OK
OGLE-SMC-ACEP-02	F	0.83	7.87 ± 0.17	0.923 ± 0.010	1.070 ± 0.011	0	0	ok
OGLE-SMC-ACEP-03	1O	0.76	6.67 ± 0.46	0.755 ± 0.015	0.765 ± 0.022	0	0	OK
OGLE-SMC-ACEP-04	F	0.83	8.23 ± 0.32	1.046 ± 0.012	1.210 ± 0.019	0	0	ok
OGLE-SMC-ACEP-05	1O	0.70	6.78 ± 0.25	0.870 ± 0.011	0.928 ± 0.013	0	0	ok
OGLE-SMC-ACEP-06	F	1.26	9.12 ± 0.68	0.824 ± 0.018	0.820 ± 0.027	0	0	OK
OGLE-SMC-T2CEP-001	pWVir	11.87	43.32 ± 1.89	1.785 ± 0.029	1.685 ± 0.040	0	0	OK
OGLE-SMC-T2CEP-002	BLHer	1.37	7.64 ± 0.67	0.484 ± 0.012	0.434 ± 0.014	0	0	OK
OGLE-SMC-T2CEP-003	WVir	4.36	12.73 ± 1.28	0.347 ± 0.011	0.278 ± 0.011	0	0	
OGLE-SMC-T2CEP-004	WVir	6.53	19.98 ± 2.56	0.569 ± 0.022	0.511 ± 0.028	0	0	OK
OGLE-SMC-T2CEP-005	WVir	8.21	19.41 ± 0.45	0.400 ± 0.010	0.326 ± 0.010	0	0	
OGLE-SMC-T2CEP-006	BLHer	1.24	7.33 ± 0.15	0.485 ± 0.010	0.459 ± 0.010	0	0	OK
OGLE-SMC-T2CEP-007	RVTau	30.96	77.35 ± 18.57	2.058 ± 0.750	1.804 ± 0.865	0	1	OK
OGLE-SMC-T2CEP-008	BLHer	1.49	10.45 ± 0.44	0.838 ± 0.011	0.913 ± 0.015	0	0	ok
OGLE-SMC-T2CEP-009	BLHer	2.97	12.97 ± 0.58	0.572 ± 0.010	0.547 ± 0.011	0	0	OK
OGLE-SMC-T2CEP-010	pWVir	17.48	60.53 ± 6.25	2.347 ± 0.226	2.296 ± 0.360	0	1	OK
OGLE-SMC-T2CEP-011	pWVir	9.93	38.92 ± 2.65	1.891 ± 0.068	1.665 ± 0.089	1	0	OK
OGLE-SMC-T2CEP-012	RVTau	29.22	41.67 ± 1.15	0.486 ± 0.010	0.352 ± 0.010	0	0	
OGLE-SMC-T2CEP-013	WVir	13.81	25.27 ± 0.67	0.386 ± 0.010	0.293 ± 0.010	0	0	
OGLE-SMC-T2CEP-014	WVir	13.88	23.85 ± 0.59	0.335 ± 0.010	0.247 ± 0.010	0	0	
OGLE-SMC-T2CEP-015	BLHer	2.57	12.70 ± 1.04	0.767 ± 0.018	0.649 ± 0.021	0	0	
OGLE-SMC-T2CEP-016	BLHer	2.11	10.22 ± 0.63	0.520 ± 0.011	0.487 ± 0.012	0	0	OK
OGLE-SMC-T2CEP-017	BLHer	1.30	8.79 ± 0.97	0.697 ± 0.024	0.703 ± 0.040	0	0	OK
OGLE-SMC-T2CEP-018	RVTau	39.52	57.52 ± 6.83	0.742 ± 0.031	0.531 ± 0.027	1	0	
OGLE-SMC-T2CEP-019	RVTau	40.91	50.40 ± 2.09	0.541 ± 0.010	0.347 ± 0.010	1	0	
OGLE-SMC-T2CEP-020	RVTau	50.62	50.15 ± 3.50	0.376 ± 0.010	0.243 ± 0.010	0	0	
OGLE-SMC-T2CEP-021	BLHer	2.31	8.99 ± 0.37	0.344 ± 0.010	0.294 ± 0.010	0	0	
OGLE-SMC-T2CEP-022	BLHer	1.47	7.22 ± 0.57	0.364 ± 0.011	0.331 ± 0.011	0	0	OK
OGLE-SMC-T2CEP-023	pWVir	17.68	39.21 ± 1.69	0.820 ± 0.011	0.670 ± 0.012	0	1	
OGLE-SMC-T2CEP-024	RVTau	43.96	51.41 ± 3.24	0.506 ± 0.011	0.326 ± 0.010	1	0	
OGLE-SMC-T2CEP-025	pWVir	14.17	30.97 ± 1.42	0.624 ± 0.011	0.496 ± 0.011	0	1	
OGLE-SMC-T2CEP-026	BLHer	1.70	10.17 ± 0.39	0.696 ± 0.011	0.680 ± 0.011	0	0	OK
OGLE-SMC-T2CEP-027	BLHer	1.54	7.70 ± 0.31	0.408 ± 0.010	0.368 ± 0.010	0	0	OK
OGLE-SMC-T2CEP-028	pWVir	15.26	49.73 ± 1.33	1.653 ± 0.014	1.655 ± 0.018	0	1	OK
OGLE-SMC-T2CEP-029	RVTau	33.68	91.49 ± 2.38	2.547 ± 0.025	2.524 ± 0.035	0	1	OK
OGLE-SMC-T2CEP-030	BLHer	3.39	14.97 ± 0.81	0.750 ± 0.012	0.658 ± 0.014	0	0	ok
OGLE-SMC-T2CEP-031	WVir	7.90	20.76 ± 2.32	0.491 ± 0.015	0.419 ± 0.017	0	0	
OGLE-SMC-T2CEP-032	WVir	14.25	26.57 ± 1.75	0.434 ± 0.011	0.320 ± 0.010	1	0	
OGLE-SMC-T2CEP-033	BLHer	1.88	11.56 ± 0.67	0.831 ± 0.014	0.831 ± 0.019	0	0	OK
OGLE-SMC-T2CEP-034	WVir	20.12	36.42 ± 1.09	0.566 ± 0.010	0.442 ± 0.010	0	0	
OGLE-SMC-T2CEP-035	WVir	17.18	29.80 ± 3.18	0.437 ± 0.013	0.326 ± 0.013	1	0	
OGLE-SMC-T2CEP-036	BLHer	1.09	9.38 ± 0.36	1.018 ± 0.012	1.117 ± 0.017	0	0	ok
OGLE-SMC-T2CEP-037	BLHer	1.56	10.03 ± 0.41	0.737 ± 0.011	0.757 ± 0.012	0	0	OK
OGLE-SMC-T2CEP-038	pWVir	4.44	21.40 ± 1.62	1.203 ± 0.035	1.152 ± 0.053	0	0	OK
OGLE-SMC-T2CEP-039	BLHer	1.89	11.52 ± 0.25	0.783 ± 0.010	0.818 ± 0.010	0	0	OK
OGLE-SMC-T2CEP-040	WVir	16.11	29.73 ± 3.47	0.465 ± 0.015	0.360 ± 0.015	0	0	
OGLE-SMC-T2CEP-041	RVTau	29.12	37.67 ± 1.72	0.400 ± 0.010	0.267 ± 0.010	0	0	
OGLE-SMC-T2CEP-042	BLHer	1.49	8.54 ± 0.18	0.544 ± 0.010	0.521 ± 0.010	0	0	OK
OGLE-SMC-T2CEP-043	RVTau	23.74	41.40 ± 2.07	0.620 ± 0.011	0.484 ± 0.011	0	0	